REPUBLIC OF TURKEY
ADANA ALPARSLAN TÜRKEŞ SCIENCE AND TECHNOLOGY UNIVERSITY

GRADUATE SCHOOL OF NATURAL AND APPLIED SCIENCES
DEPARTMENT OF BIOENGINEERING

METHODS FOR INCREASING ACCURACY IN MODELLING METAL ORGANIC FRAMEWORKS

ALİ SALİH KURT
MASTER OF SCIENCE

ADANA, 2022

REPUBLIC OF TURKEY
ADANA ALPARSLAN TÜRKEŞ SCIENCE AND TECHNOLOGY UNIVERSITY

GRADUATE SCHOOL OF NATURAL AND APPLIED SCIENCES
DEPARTMENT OF BIOENGINEERING

METHODS FOR INCREASING ACCURACY IN MODELLING METAL ORGANIC FRAMEWORKS

ALİ SALİH KURT
MASTER OF SCIENCE

SUPERVISOR
ASSOC. PROF. DR. YELİZ GÜRDAL DURĞUN

ADANA, 2022

I hereby declare that all information in this thesis has been obtained and presented in accordance with academic rules and ethical conduct. I also declare that, as required by these rules and conduct, I have fully cited and referenced all information that is not original to this work.

Ali Salih KURT

ABSTRACT

METHODS FOR INCREASING ACCURACY IN MODELLING METAL ORGANIC FRAMEWORKS

Ali Salih KURT

Department of Bioengineering

Supervisor: Assoc. Prof. Dr. Yeliz Gürdal DURĞUN

February 2022, 77 pages

High throughput screening of metal organic frameworks (MOFs) for gas mixture separations have produced large amounts of data. Reported gas permeabilities have been mainly calculated using an approximate approach. Permeability predictions of an alternative method (new method) have shown to significantly improve the predictions of the approximate method for noble gas mixtures. Permeabilities calculated using Onsager coefficients, detailed method, are accepted as correct answers, however constructing Onsager coefficient matrix is computationally cumbersome and not feasible especially for the high throughput screenings. Thus, new or approximate methods have been applied for calculating permeability and permeation selectivities of gas mixtures. However, permeability prediction accuracies of these methods for gas mixtures having dispersion and electrostatic interactions with the pores have not been discussed in the literature so far. In the first part of this thesis, we question the accuracy of permeability predictions for CO_2, H_2, CH_4 mixtures. Another perspective to increase the accuracy for screening MOFs is to determine the best net atomic charge calculation method. Density Derived Electrostatic and Chemical Charges (DDEC) method relies on optimizing the atomic electron density distribution to assign a chemically meaningful atomic charges. The method is considered to be the most reliable method, however it is computationally demanding. Non-DFT based Extended Charge Calculation (EQeq) method which is developed as an extended version of the Charge Equilibration Method assigns atomic charges by just requiring a reasonable assumption for the charge centre to compute all the ionization energies of electrons. In the second part of the thesis, we investigate the accuracy of charges assigned via EQeq with respect to the charges assigned using DDEC and discuss which method should be used for modelling MOFs.

Keywords: Gas Adsorption, Diffusion, Permeability, Molecular Dynamics, Grand Canonical Monte Carlo Simulations, Charge Assignment Methods.

ÖZET

METAL-ORGANİK KAFESLERİN MODELLENMESİNDE DOĞRULUĞU ARTTIRMA YÖNTEMLERİ

Ali Salih KURT

Biyomühendislik Bölümü

Danışman: Doç. Dr. Yeliz Gürdal DURĞUN

Şubat 2022, 77 sayfa

Metal Organik Kafeslerin, gaz karışımı ayrımları için yüksek verimli taranması büyük miktarda veri üretmiştir. Raporlanmış gaz geçirgenlikleri genel olarak yaklaşık yöntem kullanılarak hesaplanmıştır. Alternatif bir yöntemin (yeni yöntem) geçirgenlik tahminleri, soy gaz karışımlarında yaklaşık yöntemin tahminlerini önemli ölçüde iyileştirdiği gösterilmiştir. Onsager katsayılarını kullanan ayrıntılı yöntemin gaz geçirgenliklerini yüksek doğrulukta hesapladığı kabul edilir, ancak Onsager katsayı matrisini oluşturmak, hesaplama açısından zahmetlidir ve özellikle yüksek verimli tarama çalışmaları için uygun değildir. Bu nedenle gaz karışımlarının geçirgenlik ve geçirgenlik seçiciliklerini hesaplamak için yeni veya yaklaşık yöntemler uygulanmıştır. Ancak, gözeneklerle dispersiyon ve elektrostatik etkileşime sahip gaz karışımları için bu yöntemlerin geçirgenlik tahminlerinin doğruluğu şimdiye kadar literatürde tartışılmamıştır. Tezimizin ilk bölümünde CO_2, H_2, CH_4 karışımları için geçirgenlik hesaplamalarının doğruluğu sorgulanacaktır. MOF'ları taramada doğruluğu artırmak için başka bir yöntem, en iyi atomik yük hesaplama yöntemini belirlemektir. Yoğunluktan Türetilen Elektrostatik ve Kimyasal Yükler (DDEC) yöntemi, kimyasal olarak atomik yükler atamak için elektron yoğunluk dağılımının optimize edilmesine dayanmaktadır. Yöntem en güvenilir yöntem olarak kabul edilmektedir, ancak bu yöntem hesaplama açısından zorludur. Yük Dengeleme Yönteminin genişletilmiş bir versiyonu olan Yoğunluk Fonksiyon Teorisi (DFT) tabanlı olmayan Genişletilmiş Yük Hesaplama (EQeq) Yöntemi ise, elektronların tüm iyonizasyon enerjilerini hesaplamak için makul bir yük merkezi varsayımı gerektirerek atomik yükleri atamaktadır. Tezimizin ikinci bölümünde, EQeq aracılığıyla atanan yüklerin DDEC kullanılarak atanan yüklere göre doğruluğu araştırılmıştır ve MOF'ları modellemek için hangi yöntemin kullanılması gerektiği tartışılmıştır.

Anahtar Kelimeler: Gaz Adsorpsiyonu, Difüzyon, Geçirgenlik, Moleküler Dinamik, Grand Kanonik Monte Carlo Simülasyonları, Yük Atama Yöntemleri.

ACKNOWLEDGEMENTS

As I am finishing my master thesis I feel proud and thankful at the same time. The journey of completing this thesis was not easy but brought me some incredibly talented and caring teacher and the most enjoyable group of friends to work with. Here I send my best wishes to my advisor Assoc. Prof . Yeliz Gürdal Durğun for always being there to share her knowledge and pave the way for all of her students and my dear friends Behra Cantürk, Zekiye Eraslan and Gülay Akköse, who thought me a lot in a very gentle and friendly way. If I did not accomplished anything but tried to be the same good friend and student as they were to me.

Also special thanks to my family who was always patient with me during my long and sometimes stressful times spent on computer, especially Sinem Kurt, Ecem Reyhan and Cansu Ercan who endured and bring joy to me anytime I need it. This thesis made me feel like capable of something, I hope it could be a tiny drop of water that creates the ocean of science and courage people to make a better studies to enhance the quality of life on earth.

TABLE OF CONTENTS

LIST OF FIGURES

LIST OF TABLES

NOMENCLATURE

ε	energy
k_B	Boltzmann constant
c	concentration
∇c	concentration gradient
p_i	probability of a system in an i th state
p	momenta of particles
P	permeability
q	molecular partition function
Q	canonical partition function
r	coordination of particles
S_{perm}	permeation selectivity
S_{ads}	adsorption selectivity
S_{diff}	diffusion selectivity
t	time
T	temperature
U	total potential energy
V	simulation volume
v	velocity
y	bulk gas composition
δt	time step
f	fugacity
F	force
Γ	thermodynamic correction factor
d	space dimension
D	transport diffusivity
D_0	corrected diffusivity
D_s/D_{self}	self-diffusivity
D_{ii}	self exchange diffusivity of specie i corr
D_{ij}	binary exchange diffusivity
L_{ij}	Onsager's phenomenological coefficient

m	mass of a particle
n	gas uptake
j	molecular flux
J	mass flux
σ	entropy production
μ	chemical potential
Δμ	chemical potential gradient
φ	porosity
MOFs	Metal Organic Frameworks
Bio-MOFs	Biological Metal Organic Frameworks
GCMC	Grand Canonical Monte Carlo
MD	Molecular Dynamics
LJ	Lennard-Jones Potential
PLD	pore limiting diameter
LCD	largest cavity diameter
DFT	Density Functional Theory
DDEC	Density Derived Electrostatic and Chemical Charges
EQeq	Extended Charge Equilibration
CBAC	Connectivity Based Atom Contribution Charge Method

1. INTRODUCTION

Due to oil, coal and gas burning activities, our planet has been grappling with the most gas pollution and waste ever in recent years (Panahi et al., 2018). Research and development studies have been going on for years to get rid of the harmful effects of industrial applications and various chemicals that threaten human life and environment. Among them, high-throughput screening of nanoporous materials which enable rapid sorting of material performances for specific applications has gained significant attention recently. Since the methods that aim to separate and purify pollutants are difficult, expensive and require a lot of energy to carry out, new porous membrane materials have begun to be developed (Gurdal & Keskin, 2016). Using Metal Organic Frameworks (MOFs) which have been very popular in recent years, can be considered as the most common efforts introduced to the literature (Panahi et al., 2018). MOFs, which are a subclass of coordination polymers and made of crystalline metal clusters linked with organic binders, became one of the most important gas separation materials with their high quality performance. This performance leans on its unique properties such as chemical and mechanical stability, customization of pore sizes, large void volumes varying between 30% and 90% and large surface areas ranging between 1000 and 10000 m^2/g (Gurdal & Keskin, 2016).

The combination of a variety of metal oxides and the clever selection of organic binders lead to the creation of millions of MOFs with different topologies. This tailorability of MOFs allow rational adaptation of pore size, volume, and functionality for designable frameworks, thus scientists have had remarkable success in designing and applying them in many industrial applications such as adsorbents or membranes for the separation of gas contaminants (Atci & Keskin, 2012b).

Several databases on MOFs, e.g. the Computation-Ready Experimental Metal-Organic Framework Database (CoRE-MOF) (Chung et al., 2019), Cambridge Structural Database non-disordered MOF subset (CSDSS DB), and MOF database generated by Topologically Based Crystal Constructor (ToBaCCo) (Colón, Gómez-Gualdrón, & Snurr, 2017), are available for facilitating high-throughput screening of the MOFs, especially for gas separation applications.

In this respect, screening studies deposit large amounts of data to the literature related to gas permeabilities and permeation selectivities of MOFs which are used to decide which MOF outperforms one another for purification of desired gas species (Avci, Velioglu, & Keskin, 2018).

The most comprehensive method for computationally predicting transport performances of the nanoporous materials is provided by Sanborn and Snurr (Sanborn & Snurr, 2001) which will be named as detailed method throughout this thesis. Their method gives the most accurate results for gas permeabilities. However, calculating gas permeabilities using the detailed method is computationally demanding, since it requires the construction of Onsager coefficient matrix which relates driving forces with the gas fluxes in irreversible processes (Hwang, 2004; Onsager, 1931). Calculated Onsager coefficients are then used for calculating the transport diffusivities. Permeability calculations using an approximate method, suggested by Krishna and van Baten (Rajamani Krishna & van Baten, 2010), requires computing self diffusivities of the gas species instead of calculating Onsager coefficients and transport diffusivities. This simplified approach has been applied for screening the permeation selectivities of zeolite membranes for equimolar mixtures of CO_2/H_2, CO_2/CH_4, and CO_2/N_2. Later, this approximation was modified for calculating permeation selectivities of gas mixtures having arbitrary gas compositions (Keskin & Sholl, 2009) and have been widely used in the literature for high throughput screening of the nanoporous materials. For instance, Qiao et al. (Qiao, Xu, & Jiang, 2018) screened 4764 MOFs for a single-step separation of CO_2 and N_2 from a $CO_2/N_2/CH_4$ mixture. The approximate method was used for predicting permeabilities and permeation selectivities and comparisons identified seven best MOFs for separating CO_2 and N_2 from the three component mixture. Glover and Besley (Glover & Besley, 2021)estimated membrane based separation performances of 1183 MOFs for equimolar mixtures of CO_2/CH_4 and H_2S/CH_4 using the approximate method. Altintas et al. (Altintas et al., 2018) compared the H_2/CH_4 separation performances of 4240 MOF membranes and they identified the top ten best performing MOFs which can separate the components effectively. Daglar et al. (Daglar, Erucar, & Keskin, 2021) screened 5629 MOF membranes and 78,806 MOF/polymer mixed matrix membranes for diffusion based separation of O_2/N_2 mixture using the approximate approach.

Gurdal and Keskin proposed one another method, called a new method, for calculating permeabilities and permeation selectivities of MOF membranes for binary gas mixtures (Gurdal, 2021; Gurdal & Keskin, 2016). Incorporating thermodynamic correction factors in the new method has significantly improved the predictions of the approximate method. The new method has been tested for predicting permeabilities of noble gas mixtures, Xe/Kr and Xe/Ar, and results have shown astonishing resemblance with the detailed method especially for the MOFs having larger pore sizes. Introducing thermodynamic correction factors in the new method has significantly improved the predictions of the approximate method and become an alternative method for determining membrane based separation performances of the nanoporous materials.

So far the new method has been only applied for determining the noble gas permeabilities of the MOFs (Gurdal, 2021; Gurdal & Keskin, 2016). Interactions of the noble gases with the MOF pores have been modeled considering only Lennard Jones potential and the selected noble gases, Xe, Kr, and Ar, have similar energy parameters and sizes. The accuracy of the approximate and new method predictions for gas mixtures having different sizes and having also electrostatic interactions with the MOF pores have not been discussed in the literature so far. Accurate predictions of the industrially important gas mixture permeabilities, such as H_2/CH_4 and CO_2/H_2, is crucial for proper leading of the experimental studies as well as industry towards CO_2 capture, H_2 or CH_4 purification. As aforementioned studies suggest widely applied approximate method can show significant deviations from the real permeability values calculated using the detailed method, which for sure raises reliability concerns for the results of the high-throughput screening studies using the approximate method. In this work, we question the accuracy of the permeability values calculated using the approximate and new methods by comparing the results with the ones that were calculated using the detailed method. Zeolitic imidazolate frameworks (ZIFs) which are a sub-class of MOFs and show topological isomorphism with the zeolites (Banerjee et al., 2008; Park et al., 2006) are chosen as membrane medium. Permeabilities of H_2/CH_4 and CO_2/H_2 mixtures have been investigated in several ZIFs, namely ZIF-6, ZIF-10, ZIF-60, ZIF-69, ZIF-79, and ZIF-81, which have different topological and chemical features. Adsorption loadings of the gases at several feed pressures are calculated using the Grand Canonical Monte Carlo (GCMC)

simulations. Calculated loadings are used in the Molecular Dynamics (MD) simulations as initial states for determining permeabilities using the detailed method. Permeabilities are then compared with the predictions of the approximate and new methods. While the permeabilities of the new method has been compared with the approximate and detailed methods only for noble gas mixtures so far, our present work takes previous studies one step further and investigates the predictions of the approximate and new methods for gas mixtures having different sizes and/or having electrostatic interactions with the MOF pores in addition to the dispersion forces.

Another crucial step to successfully screen MOFs is the assignment of the net atomic charges in the structure. All the net atomic charge calculation methods try to replace the complicated function of the electron density in materials which are responsible for almost all of the properties of the materials. It gives all atoms of the material a charge value to make it easy to use that materials in simulations (Manz & Sholl, 2010). Atomistic simulations that use this data are based on interatomic interactions which are strongly depending on the charges of the atoms (Manz & Sholl, 2010). These kinds of simulations commonly used in modelling of complex materials and provide significant information such as charge transfer and adsorption performances. And due to partial charges are derived from electron density of the related material, e.g. MOFs, even small chemical difference between MOFs, could cause distinct charges and hence, significantly affect the process that the material used in.

There are multiple approaches for this purpose which have different principle based on the theory they use. Bader's method, for instance, needs low computational cost to analyse charges from quantum chemistry based pre-defined charge density but fails to accurately create the electrostatic potential energy surface (EPES) within a periodic structure (*Atoms in Molecules*, 1994). Repeating electrostatic potential extracted atomic (REPEAT) method developed by Krykunov and co-workers to fit an electrostatic density implementing Density Functional Theory (DFT) (Krykunov, Demone, Lo, & Woo, 2017). The method proved to be one of the most reliable methods as well as Density Derived Electrostatic and Chemical Charges (DDEC) method, however, studies showed that REPEAT method sometimes reproduce unphysical charges (Watanabe, Manz, & Sholl, 2011). Xu and Zhong proposed

Multilayer Connectivity-based atomic charge (m-CBAC) approach that employs atom's three bond connectivity levels; 2^{nd}, 1^{st}, and 0^{th}, respectively and assigns a charge for each pattern of connectivity (Changlong Lin, Penley, Cho, & Lin, 2020). After that, an atomic charge assigned for each atom of the MOF depend on the connectivity pattern followed by 2nd-layer, 1st-layer and 0th-layer, respectively where the accuracy of the charge is decay at each level. At final, the method shows its best performance only on the materials with same boding environment.

Density Derived Electrostatic and Chemical (DDEC) method is based on Density Functional theory, thus considered to be one of the most reliable charge assignment method in the literature (Manz & Sholl, 2010). Manz and Sholl developed this charge partitioning method to assign charges outside of the electron distribution by spherical averaging of the ion densities provided by DFT calculations. One another method, Extended Charge Equilibration (EQeq) method, on the other hand, uses approximations instead of considering electron densities around atoms, hence has a potential to deviate from the charges calculated using DDEC (Wilmer, Kim, & Snurr, 2012). Despite the variety of the charge assignment methods there is still an ambiguity in defining point charges of nanoporous materials. As a second part of this thesis, we aim to compare the results of two charge assignment methods and determine the deviation of the EQeq method with respect to the DDEC. This will enable us to determine more accurate charge method that should be used for modelling the MOFs.

2. LITERATURE REVIEW

MOFs can be used at numerous applications including gas capturing, gas separation, electrochemical energy storage, sensing, catalysis, and in the production of inorganic functional materials. While type of MOFs can be almost limitless due to tailorability of their organic and inorganic parts, molecular simulation methods gain a great importance by being greatly time efficient on determining advantageous properties of MOFs in different application areas. Therefore, investigation of the adsorption properties of MOFs usually unites with molecular modelling techniques.

In this part the literature review of the studies that deals with the gas separation performances of MOFs are summarized. The summary is going to cover especially separation of CO_2/H_2 and CH_4/H_2 gas mixtures through a zeolitic imidazolate framework (ZIF) membranes via both experimental and molecular modelling. Additionally, studies using DDEC or EQeq charges in molecular simulations are reviewed.

2.1. Studies on Gas Separation with MOFs and ZIFs

Yaghi and co-workers were the first to synthesize MOFs and indicated that they are remarkably convenient for gas adsorption and purification systems (Yaghi, Li, & Li, 1995). Zeolite Imidazolate Frameworks (ZIFs) which are topologically isomer to zeolites due to their tetrahedral networks between transition metals and imidazolate ligands, are considered to be a subclass of MOFs (Atci & Keskin, 2012a). Co-polymerization of Zn and Co transition metals with an imidazolate type linker leads to the production of a ZIF, where (Zn/Co)-Im-(Zn/Co) bonds occur between organic and inorganic parts of the material (Atci & Keskin, 2012a). This bound has the same angle as the Si-O-Si bond present in zeolites which makes ZIF structures to resemble zeolites (Atci & Keskin, 2012a). Yet, ZIFs are more advantageous where they go through a relatively easy production and can be produced diversely as MOFs do (Atci & Keskin, 2012a). Therefore various products bring on a wide range of application areas by modifying the structure of the material by adjusting the organic and inorganic parts (Atci & Keskin, 2012a).

Taking into consideration that there is large body of synthesized MOFs and ZIFs, it is so demanding to define their properties and performances by carrying out only experimental studies. However, novel computational simulation methods are assisting excellently to comprehend adsorption and separation skills of new porous materials in detail.

Using membranes in the technologies for the separation of industrial gases is a promising method, as reported in the literature (Gurdal, 2021). These kinds of processes are 90% more energy efficient and notably requires less cost compared to other distillation based adsorption methods (Abdul Hamid et al., 2021). In addition, porous membrane systems that can be operated both stand-alone and readapt to the existing unit of the system, induce less carbon to the atmosphere and has the ability to adjust in every step of scale up (Abdul Hamid et al., 2021). Among these membranes based systems zeolites, ceramic membranes such as aluminium oxide and a novel and promising class of porous materials; MOFs are the most useful ones.

One of the early uses of molecular modelling study is reported by Maginn and co-workers in 1993, equilibrium molecular dynamics (EMD), non-equilibrium molecular dynamics (NEMD) and Darken model were applied for calculating CH_4 diffusion in silicate zeolites (Maginn, Bell, & Theodorou, 1993). This study defined EMD as a promising method when the system has a continuously linear response (Maginn et al., 1993). Düren et al. (Düren, Sarkisov, Yaghi, & Snurr, 2004) modelled a simulation for predicting effect of many physical features of nano porous materials including MOFs on the CH_4 adsorption amount. The conclusion of their study indicated that CH_4 adsorption would be more efficient by using MOFs with large surface area, low framework density, high free volume, and strong CH_4-adsorbent interactions (Düren et al., 2004). After that, the same phenomenon examined by applying a molecular simulation that uses variety of MOFs with organic linkers having different lengths, e.g. IRMOF-1, IRMOF-8, IRMOF-10, IRMOF-14, IRMOF-16. As study suggests, the ones with longer organic linkers captured more CH_4 at multiple pressure points (Düren & Snurr, 2004).

Another perspective was to determine if the catenation on MOFs enhance the H_2 adsorption where Grand Canonical Monte Carlo (GCMC) revealed that the creation of small pores in the

catenated IRMOFs retain more H_2 than non-catenated ones (Jung et al., 2006). Then, Han et al. tried to understand the effect of functional groups in the MOFs and ZIFs on H_2 adsorption at 300K and 77K at various pressures (Han, Choi, & Goddard, 2010). As a result, ZIFs with high surface area and small pore diameters lead to more H_2 adsorption where low pressures increase the H_2 binding energies and so the adsorption amount, where high pressures diminish available adsorption sites and the H_2 storage.

MOFs have been also studied for the adsorption of other gas mixtures including industrial ones. As an example, Krishna et al. used a Monte Carlo simulation in order to examine CO_2/H_2, CO_2 /CH_4, and CH_4/H_2 gas mixture separation performances of a material called MgMOF-74 (Rajamani Krishna & van Baten, 2010). Simulations agreed that while increasing concentration of gases in the system causes more interactions between molecules, separation performance of the framework also improves.

Krishna and Baten (Rajamani Krishna & van Baten, 2010) investigated separation characteristics of various MOFs and traditional adsorbents for the separation of CO_2/CH_4, CH_4/H_2, CO_2/N_2, and CO_2/H_2 gas mixtures. They used Configurational-Biased Monte Carlo Simulation (CBMC) and MD simulations and calculated the adsorption selectivity, the working capacity, diffusion selectivity, and membrane permeability of many MOFs. Among them MgMOF-74 served as the best CO_2 capture and had highest permeabilities, permeation selectivity, and working capacity on CO_2/N_2, CO_2/H_2, and CH_4/H_2 mixtures. In addition, MgMOF-74 and ZnMOF-74 noted to be promising membrane separation materials for CH_4/H_2 mixtures owing to offering high selectivity values. In one of their another study, they reported that ZIF-8 would be more efficient as a membrane for separating CO_2/H_2 mixture (Rajamani Krishna & van Baten, 2010).

Yang et al. used GCMC simulations to determine CO_2 separation performance of CuBTC from mixtures of CO_2/N_2 and CO_2/N_2 at different gas compositions and temperatures and reported that these factors are as significant as the bulk pressure of the system (Yang, Xue, Zhong, & Chen, 2007). Couple years later, Guo and co-workers simulated a system in order to predict adsorption and separation of CH_4/H_2 mixtures in five ZIFs (Guo, Shi, Ma, & Liu,

2010). They concluded that CH_4 molecules adsorbed more than H_2 molecules at both single and mixture components and high adsorption rates have been observed in the close vicinity of the organic linkers which indicates that topology of the framework affects selectivity (Guo et al., 2010).

Concordantly, Jiang et al. investigated performances of several MOFs for CO_2 uptake (C. Zheng, Liu, Yang, Zhong, & Mi, 2009). They chose specific MOFs which differ from each other as topology, pore size and chemical characteristics which lead to a conclusion that framework structure is significant criteria for CO_2 adsorption at low pressures, however results does not hold at higher pressure rates. After that, Babarao and co-workers investigated CO_2/CH_4 adsorption and separation process by using MOFs with different exposed metals, catenation and extra framework ions which showed that these properties slightly enhance CO_2 selectivity over CH_4 (Babarao, Jiang, & Sandler, 2009). Babaora and Jiang studied rho zeolite-like metal organic frameworks (rho-ZMOF)'s ability to separate CO_2/H_2, CO_2/CH_4, and CO_2/N_2 mixtures and obtained promising results where rho-ZMOF uptakes more CO_2 with respect to the other materials under consideration owing to its highly charged framework along with Na^+ ions that act as an extra framework (Babarao et al., 2009).

Atci and co-workers (Atci, Erucar, & Keskin, 2011) reported another research that deals with the separation of CH_4, CO_2, H_2 mixtures in Bio-MOF-11 which has a simple biomolecule as an organic linker and biocompatible metal cation in its structure. Bio-MOF-11 appeared to have remarkably high adsorption selectivity for CO_2 (Atci et al., 2011). The same authors also simulated adsorption performances of various ZIFs for CH_4, CO_2, H_2, and N_2 components as well as H_2/CO_2, H_2/N_2, H_2/CH_4 mixtures and compared simulation results with experimental studies which agree well with each other (Atci & Keskin, 2012a).

Keskin reported two different studies at 2010 that uses atomically detailed simulations where the first study compared isostructural MOFs with various metal sites, as a membrane for CH_4/H_2 mixture separation and the other used couple of ZIFs for separation of CH_4/H_2, CO_2/CH_4, and CO_2/H_2 mixtures (Keskin, 2010). Simulation results of the first study predicted those MOFs adsorb more gases and more selective than IRMOFs (Keskin, 2010, 2011).

Second study determined that ZIF-3 and ZIF-10 have highest adsorption selectivities than common MOF membranes (IRMOF-1-8-10-14) for all introduced gas mixtures (Keskin, 2010). One of the most recent studies concerning MOFs is reported by Keskin et al. (Altintas & Keskin, 2019)where they applied GCMC simulations and investigated 3794 MOFs to predict their CO_2/CH_4 separation performance and decided on top 8 MOFs with best CO_2 permeabilities ($>10^6$ Barrer) and many MOFs that have promising CO_2/CH_4 selectivity larger than 80.

Concerning the ZIFs, they have been first introduced to the literature by Park et al. (Park et al., 2006). In the means of gas separation performances of ZIFs, a large number of studies have been reported as MOFs. Liu et al. investigated separation ability of ZIF-69 when it is exposed to CO_2/CO mixture and they compared diffusion and adsorption capacities of various ZIFs in the presence of CO_2 /CH_4, CH_4/H_2, CO_2/H_2, and CO_2/N_2 mixtures using molecular simulations (Battisti, Taioli, & Garberoglio, 2011; Chokbunpiam et al., 2016; Y. Liu, Hu, Khan, & Lai, 2010). Another noteworthy research published in 2008, examining CO_2 storing performances of ZIF-95 and ZIF-100 from CO_2/CH_4, CO_2/N_2 or CO_2/CO syngas mixtures (Wang, Côté, Furukawa, O'Keeffe, & Yaghi, 2008) . Zeeshan et al. analysed the CO_2 separation of ZIF-8 as an adsorbent and concluded that ZIF-8 gives promising results (Zeeshan et al., 2018).

Another comprehensive research studying wide range of ZIF materials in order to understand potential on gas separation processes is reported by Atci and Keskin at 2012 (Atci & Keskin, 2012b). The investigators employed a simulation method in order to examine adsorption and separation based selectivity and gas permeabilities of 15 different ZIFs on CH_4/H_2, CO_2/CH_4, and CO_2/H_2 mixtures (Atci & Keskin, 2012b). The results indicated that ZIF-2, ZIF-69, ZIF-79, ZIF-81, and ZIF-90 can be more preferable than the common MOFs and zeolites. All of these studies used molecular simulation systems to predict adsorption based performance, yet membrane based adsorption performances of ZIFs have not been widely analysed.

Battisti et al. (Battisti et al., 2011) used similar molecular dynamic simulations to track permeation selectivity of ZIF-2, ZIF-4, and ZIF-8 towards CO_2/H_2, CH_4/H_2, CO_2/CH_4,

CO_2/N_2, and CH_4/N_2 industrial syn-gas mixtures at different temperatures . An article written by Atci and Keskin, aimed to model gas transport mechanism of gas mixtures with molecular models using ZIF-90 and ZIF-65 membranes along with ZIF/Polymer Composite Membranes (Atci & Keskin, 2012a). Same researchers go further and investigated potential of plenty ZIF's adsorption and membrane based separations on CH_4/H_2, CO_2/CH_4, and CO_2/H_2 mixtures in detail by performing atomically detailed simulations and predicted several ZIFs membranes having higher selectivity and permeability (Atci & Keskin, 2012b).

2.2. Studies Employing Permeability and Permeation Selectivity Calculation Methods

Detailed method of Sanborn and Snurr is successfully incorporated in the large body of studies that question the membrane performance of MOFs and variety of nanoporous materials (Rajamani Krishna & Baten, 2011; Zeng, Liu, & Liu, 2018). Keskin studied adsorption and membrane based separation of CH_4/H_2, CO_2/CH_4 and CO_2/H_2 mixtures using an rht-type metal–organic framework (MOF) and determined the gas permeability and permeation selectivity of the MOF using the detailed method (Keskin, 2013). After that Yılmaz et al. calculated adsorption and membrane based gas separation performance of numerous ZIFs by detailed method (Yilmaz, Ozcan, & Keskin, 2015). They used molecular simulation methods to simulate gas separation processes of both single component CH_4, CO_2, H_2 and N_2 and binary mixtures CO_2/CH_4 CO_2/N_2, CO_2/H_2 and CH_4/H_2 through ZIFs.

Approximate method, as being a faster and easier permeability calculation method, have been also appeared on several studies that concerns screening of MOFs or other materials for gas separation applications (Fischer, Hoffmann, & Fröba, 2012; R. Krishna & van Baten, 2007). A comprehensive research performed by Qiao and co-workers where single component separation ability of vast body of MOFs is investigated to determine the best performing MOFs using the approximate method (Qiao et al., 2018). A recent study predicted separation of binary mixtures of CO_2/CH_4 and H_2S/CH_4 of 1183 MOF membranes, reported by Glover and Besely (Glover & Besley, 2021). Altintas and co-authors employed the same permeability calculation procedure, approximate method, to test 4240 MOFs as membranes for the separation of H_2/CH_4 mixture and provided the best promising MOFs (Altintas et al., 2018,). Daglar et al. utilized approximate approach to determine the best O_2/N_2 mixture separation

membrane among libraries of MOF and MOF/polymer mixed matrix membranes (Daglar et al., 2021).

The new method proposed to the literature very recently and there are limited studies that incorporates the method into MOFs performance investigations. Gurdal et al. proposed the new method and applied to predict the Xe/Kr and Xe/Ar noble gas separation performances of 8 MOF membranes. According to their results, the new method makes better predictions than the approximate method and gives closer permeability and permeation selectivity results with the detailed methods (Gurdal & Keskin, 2016). The new method have been often used to determine the permeabilities of nobel gases in MOFs (Durğun, 2019; Gurdal, 2019; Sumer & Keskin, 2017), conversely there is no study that employs the new method on separating industrial gas mixtures, e. g. CH_4, CO_2 or H_2.

2.3. Net Atomic Charge Calculation Methods

Determining net atomic charges of the materials which are used as inputs in GCMC and MD simulations are crucial to specify the separation properties of the MOFs or ZIFs since these charges result in interactions between atoms and directly affect the adsorption and separation process (D. Li et al., 2021). For example, Walten et al. presented a study that simulates CO_2 adsorption of MOF-5 in two different GCMC simulations where Coulombic interactions only accounted in one simulation. The results of the simulation that counts electrostatic interactions between adsorbate molecules have better agreement with experimental studies (Walton et al., 2008). Likewise, the net atomic charge that employed in the computational simulations affects the interaction between CO_2 and MOF, considering CO_2 is a molecule having quadrupole moment and has electrostatic interactions which makes them as deterministic as van der Waals interactions, as Watanabe and co-workers reported (Watanabe et al., 2011). Their results showed that the effect of the calculated atomic charges which are calculated by using various methods, is generally depend on the material type in the adsorption process. For instance, some materials show the same adsorption isotherms, although different atomic charges were assigned to their atoms and there are some other materials which show significant change in their adsorption capacities with a slight difference in assigned charges.

Quantum chemistry calculations are preferred as a common approach to determine adsorbent charges using model clusters. In a typical quantum chemistry approach a model cluster or a unit cell is sectioned from each MOF structure. After that DFT computes the charge density and electrostatic field around the unit cell where this data is used to obtain atomic charges using a different method to partition the charge density (Hirshfeld, 1977) or to fit a local electrostatic field for atoms (Tan & Cheetham, 2011). However, these approaches are not completely reliable owing to the fact that the calculated charges depend on the details of unit cell which means resulted point charges may differ. It is also not suitable for periodic structures due to ignoring the periodic iteration of long-range electrostatic field in the material. Multiple approaches have been developed in order to create more direct charge assignment methods for periodic systems. Bader proposed an approach to find charge density on atoms using a method that splits the space into atomic regions by surfaces having minimum charge density. This procedure make the electron density with no component normal to the surface. Furthermore, while this surfaces often have a nucleus, sometimes a nucleus is not considered in the method. Therefore the method is insensitive to the electron wave function calculations. While the method demands so much computational effort along with having a complex algorithm on finding the dividing surfaces, Henkelmen and co-workers proposed simpler approach using the partitioning method of Bader, and aimed to decompose the electronic charge density into atomic regions. Yet, the method was not suitable for periodic systems (Henkelman, Arnaldsson, & Jónsson, 2006).

Campana et al. developed an accurate approach to achieve this purpose by fitting electrostatic field obtained by periodic DFT calculations and adjusting the point charges (Campañá, Mussard, & Woo, 2009). This method is called repeating electrostatic potential extracted atomic (REPEAT). Nevertheless, REPEAT method proved to be sensitive while defining the excluded volume by input parameters and resulting charges do not bear adequate chemical significance and reproduce reliable atomic charges only for the materials with similar bonding connectivity (Chen, Stern, Space, & Johnson, 2010).

There are also several semi-empirical charge assignment approaches in the literature such as connectivity-based atomic charge (CBAC) approach proposed by Xu and Zhong (Xu &

Zhong, 2010). It assigns the same point charges for the atoms with same bonding connectivity on the basis of their local coordination environment even for different MOFs. Training of the method was applied to 30 MOFs. The atomic charges of CBAC method gave quite similar adsorption isotherms of CO_2, CO and N_2 as the ones with quantum mechanical calculations. Unfortunately, the method is not comprehensive, since it requires materials that chemically similar with the initial training set.

Manz and Sholl introduced a method called Density Derived Electrostatic and Chemical (DDEC) at 2010 (Manz & Sholl, 2010). The method basically provides a chemically meaningful net atomic charges from a known electron density. It optimizes electrostatic potential to regenerate outside of the electron distribution by simultaneously optimizing atomic electron density distributions (Manz & Sholl, 2010). Manz and Snoll reported that DDEC method provides reliable charges for systems with zero, one, two, and three dimensions periodicity, porous and nano porous solids; solid surfaces; and both large and small molecules in a variety of materials including molecules, nano porous solids, solid surfaces, and metal organic frameworks (Manz & Sholl, 2010). They also tested validity of DDEC results by comparing with the other charge calculation methods and concluded that DDEC gave the most accurate results for large body of system types among other calculation methods (Manz & Sholl, 2010). In addition, the obtained charges exhibit good transferability between related chemical systems which makes them very suitable for the construction of force fields used in atomistic simulations (Manz & Sholl, 2010).

The DDEC method have been carried out in several studies including the one by Sholl and co-authors to develop transferable force fields to predict adsorption of H_2O in Cu-BTC (Zang, Nair, & Sholl, 2013). Haldoupis and co-workers aimed to find selective membranes among almost 500 MOFs for separation of N_2/CO_2 by assigning the right charge calculation method (Haldoupis, Nair, & Sholl, 2012). They computed charges of MOFs with validated periodic charge equilibration method (PQeq) and calculated the CO_2/N_2 selectivity. After that, they selected 11 frameworks among those having selectivity greater than 100. This selection included six frameworks with a high difference between calculated PQeq and non-charged results, and 5 frameworks that proved to stable after solvent removing process. The selectivity

results of these 11 frameworks were compared with the selectivities obtained with DDEC. However, results cleared that the selectivities calculated with PQeq and the no-load model were not close to the selectivity obtained using DDEC (Haldoupis et al., 2012).

DDEC method was used to assign point charges of eight MOFs in Erucar and co-authors study in order to observe the affect of existence of electrostatic interactions between adsorbates and several MOF atoms and MOF/polymer combinations (Erucar, Manz, & Keskin, 2014). Comparison of calculated charges gave reasonable similarity respect to the experimental data which allowed for the further investigation of CO_2/CH_4, CO_2/N_2 and H_2/CO_2 separation performances of studied materials (Erucar et al., 2014). This conclusion is interpreted as DDEC method is promising to define electrostatic interactions between CO_2 and MOF atoms.

Watanabe and Sholl studied pore characteristics and CO_2 and N_2 separation performances of large body of MOFs using classical molecular dynamics simulations (Watanabe & Sholl, 2012). Pore size analysis relies on calculation of Henry's constant which demands atomic charge calculation. They did not use net point charges but performed DFT to assign electrostatic potential energy surface (EPES) and incorporated it into simulations. Validity of the DFT-EPES procedure is tested using the MOFs with DDEC and PQeq based charges along with neutral charged MOFs to describe their electrostatic interactions in the separation of CO_2 and N_2 gases. DFT-EPES and DDEC based separation process showed great agreement as well as their charges where the closest results for DFT-EPES obtained from DDEC charges. Results indicated that PQeq charges are reliable enough for basic screening studies but PQeq based Henry's constants did not correlated well with DFT-EPES results as DDEC. Assigning less accurate charges also resulted in significant underestimations of Henry's constants. Calculation of Henry's constant using DDEC and Qeq method also investigated by Li and co-authors on the process of high-throughput computational screening for CO_2/H_2O separation performances of 15 MOFs. They concluded that DDEC and Qeq method results in similar Henry's constant for N_2 and CO_2 but their results significantly deviate from each other for H_2O where the deviation continued for the separation of CO_2/H_2O.

Deeg and co-workers observed CO_2 adsorption properties of ten ZIFs by applying three varying sets of charges of framework where only 70% of the calculated charges remained the same (Deeg et al., 2013). They investigated the effect of different framework charges on adsorption enthalpies and they were very high for ZIF-3, ZIF-7, ZIF-93, and ZIF-97 while the effect was small for ZIF-96. However, the choice of charges nearly did not effect the results of methanol adsorption on ZIF-8 as reported by Zhang et al. (Zhang, Zhang, & Jiang, 2013). Zheng et al. were the other researchers to indicate that the atomic charges obtained by REPEAT (Campañá et al., 2009), CBAC (Xu & Zhong, 2010), and DDEC (Manz & Sholl, 2010) methods, result quite different self diffusion coefficients of CO_2 in ZIF-8 (B. Zheng, Sant, Demontis, & Suffritti, 2012). Yet, DDEC and electrostatic potential derived atomic charges have provided closer results with respect to the experimental values. Liu et al. studied the same ZIF and gas composition but with a different set of charges where Lennerd-Jones potential parameters have been also changed (D. Liu & Zhong, 2010). They found two times larger self diffusion coefficient than Zheng's results which proves that electrostatic interactions have a great effect on the correct modeling of adsorption and diffusion behaviour of materials. Similar study was performed by Yang and Zhong in the case for separation of CO_2/CH_4 in MOF-199 with electrostatic interactions between adsorbent-adsorbate and adsorbate-adsorbate (Yang & Zhong, 2006). Their research demonstrated that the selectivity highly increases in the quadrupolar molecules like CO_2 and N_2 due to the electrostatic interactions resulted from a quadrupole moments inside the nano pores of the material (Yang et al., 2007).

Nazarian and co-authors computed Density Functional (DFT) derived DDEC charges of nearly 3000 experimentally synthesized MOFs and compared the results with the results obtained using the EQeq method (Nazarian, Camp, & Sholl, 2016). They concluded that using DDEC partitioning method of charges leads to well studied assessment of gas adsorption properties of MOFs while the EQeq method demonstrated drastic differences reference to the DDEC method. Recent study reported by Altintas and Keskin evaluated the role of charge assignment methods, particularly DDEC and Qeq, in large screening of MOFs for separation of CO_2/CH_4 gases (Altintas & Keskin, 2020). CO_2/CH_4 adsorption in 1500 MOFs is simulated using the DDEC and Qeq charged. The DDEC and Qeq method employed simulations

generated varying gas storage, working capacity, permeation selectivity and regenerability of MOFs. The authors also sorted two sets of the top MOFs depending on charge calculation method used and showed that the best MOF adsorbates were varying on DDEC-charged and Qeq-charged MOFs. Furthermore, the effect of charge calculation method was also examined for gas diffusion, permeability and membrane selectivity and they concluded that for the MOFs with large pore areas, the charge method choice do not cause a significant difference but the predictions of the DDEC-charged and Qeq-charged MOFs with narrow pore sized MOFs highly varied with each other. The authors ends the study by suggesting that Qeq charged screening researches are time-efficient and practical for large number of MOFs but more accurate charge assignment methods such as DDEC is obligated to present the best MOFs for adsorption processes.

EQeq uses only the initial ionization energies, but with reduced number of parameters (Anthony K. Rappe & Goddard, 1991; Wilmer, Kim, & Snurr, 2012). The method can be applied to periodic systems and does not require iterative convergence which makes it faster to determine partial charges at every MD time-step (Wilmer, et al., 2012). In order to validate charge results they also compared them with two other charge calculation methods. Grand Canonical Monte Carlo Simulations are used to demonstrate CO_2 uptake of twelve MOFs after applying EQeq method and the other methods (REPEAT and ChelpG) (Wilmer, et al., 2012). They showed that the EQeq charges are as good as charges derived from electrostatic potentials. The same authors reported one of the early used of EQeq method where they screened a library of hypothetical MOFs using molecular simulation by using partial atomic charges calculated by EQeq method (Wilmer, Farha, Bae, Hupp, & Snurr, 2012).

Snurr and co-workers worked on CO_2 capture of large body of MOFs in the presence of water (S. Li, Chung, & Snurr, 2016). The research aimed to reveal adverse affect of water in gas adsorption processes. The first step of the study covered calculation of charges using EQeq method for 5109 MOFs as well as using REPEAT method. Then, Henry's constants of each MOFs were determined. 15 MOFs with high selectivity is selected depend on the ratio of Henry's constant for CO_2 and H_2O and investigated further by molecular simulation techniques. As a result, H_2O uptake of a material proved to be highly effected by the charge

assignment method used to calculate long-ranged electrostatic potentials by comparing CO_2 and H_2O selectivities of EQeq-charged and REPEAT-charged MOFs.

Sladekova et al. studied different charge assignment methods namely DDEC (Limas & Manz, 2018), ChelpG (Breneman & Wiberg, 1990), LoProp (Gagliardi, Lindh, & Karlström, 2004), EQeq (Wilmer, et al., 2012), and REPEAT(Campañá et al., 2009) to compare adsorption isotherms of carbon dioxide and water in multiple MOFs (Sladekova et al., 2021). The comparison of charge method demonstrated that EQeq calculated the lowest charge on CuBTC, nevertheless, this variation had not a profound impact on the uptake of CO_2.

Avci et al. experimented the impact of different metal centres on CO_2/H_2 mixture separation and adsorption performance of HKUST-1 and HATGUF by performing GCMC simulations (Avci, Velioglu, & Keskin, 2019). In order to validate their simulation results with available resources, they used Qeq and EQeq method to assign charges and determine the best method that reproduces the most similar adsorption isotherms with experimental and/or computational results. As a result, they assessed which metal centre of MOFs agree with experimental results. At some cases Qeq gave more accurate adsorption isotherms than EQeq method where some metal centred MOFs with EQeq charges with +2 oxidization state also showed good agreement with experimental adsorption isotherms and DFT charge based CO_2 adsorption results such as Cr-HKUST, Ni-HKUST and ZNHKUST. This comparisons helped to conclude that the metal site has a great impact on CO_2 and H_2 adsorption. Recently, Li and colleagues studied 275 covalent−organic frameworks for adsorption heat pumps by performing Monte Carlo simulations and EQeq charge assignment method (W. Li, Xia, & Li, 2020).

As a result, DDEC is an accepted method to give the most realistic point charge results owing to consideration of electron density of the atoms in the system by quantum mechanical calculations which consume large amount of time and work. EQeq method only needs atomic positions and atomic numbers consisted in a material, hence being the fastest way among the charge assignment approaches, but also showing some drastic failures. The second part of our thesis aims to give an insight about the deviation of EQeq charges with respect to the DDEC charges for MOFs having biological linkers (Bio-MOFs).

3. THEORETICAL APPROACHES

In this chapter, we briefly introduce the theoretical background of Grand Canonical Monte Carlo and Molecular Dynamics simulations.

3.1. General Theory of Grand Canonical Monte Carlo (GCMC) Simulations

The microscopic and macroscopic properties of a system determine the state of each molecule and the thermodynamic character of the system (Frenkel & Smit, 1996). Statistical mechanics provides a framework that explains the macroscopic characteristic of a system by integrating classical and quantum-mechanical descriptions of the atoms and molecules in a system (Frenkel & Smit, 1996). While the description of the macroscopic assembly of atoms is impractical, statistical mechanics use average or highest probability results to overcome this problem.

Equation 3.1.1 uses Boltzmann distribution to describe the probability (p_i) of a system having N particles and total energy E_i at temperature T.

$$p_i = \frac{e^{-E_i/k_B T}}{\sum_{i=1}^{N} e^{-E_i/k_B T}} \quad (3.1.1)$$

where $\sum_{i=1}^{N} e^{-E_i/k_B T}$ represents the canonical partition function (Q) of the system. The canonical partition can be obtained by integrating molecular coordination of all N particles (r^N) and corresponding momentum (p^N) as shown below;

$$Q = \int dp^N dr^N e^{\frac{-E(p^N, r^N)}{k_B T}} \quad (3.1.2)$$

As atoms have different positions at each instantaneous step, we can consider any function A to represent a step and <A> to describe total instantaneous configurations of A values with the probability p;

$$\langle A \rangle = \int A.\, p(A).d(A) \quad (3.1.3)$$

By inserting partition function and the definition of the probability, Equation 3.1.3 also can be formed as;

$$\langle A \rangle = \frac{\int d\, p^N dr^N A\left(p^N, r^N\right) e^{-E\left(p^N, r^N\right)/k_B T}}{\int d\, p^N dr^N e^{-E\left(p^N, r^N\right)/k_B T}} \quad (3.1.4)$$

Computation of average of <A> would be very difficult using Equation 3.1.4. However, Monte Carlo importance sampling can be easily used as a numerical method for finding aforementioned averages.

Metropolis and co-workers introduced Monte Carlo method that enables computing the average of functions of a system by means of sampling algorithm (Metropolis, Rosenbluth, Rosenbluth, Teller, & Teller, 1953). Sampling creates ensembles which can be several different types, e.g. canonical, micro canonical, isobaric-isothermal, and grand canonical, according to represented constant external conditions or number of particles (Frenkel & Smit, 1996). To model adsorption processes Grand canonical ensemble with constant chemical potential, temperature and volume is the most relevant ensemble type since at the saturating loading adsorbed gas and the bulk gas are at equilibrium which demands constant chemical potential and temperature.

In order to achieve the lanced amount of adsorbed molecules, temperature and chemical gradient, the average number of particles in the system must be determined from the simulation (Frenkel & Smit, 1996). In this case, GCMC method is used to provide a system at fixed volume, temperature and number of particles. It simulates and records the density fluctuations of particles. This fluctuation could happen by means of five type of moves of particles including translation, rotation, insertion, deletions and identity change move. These moves are rejected or accepted whether they put the system in equilibration with lowest energy level or not using Boltzmann-type weighting. The simulation also changes pressures. After millions of trials of the system states the equilibrium amount of adsorbed molecules and

adsorption isotherms at imposed temperature, volume, and chemical gradient are determined by changing the pressure at same conditions.

3.2. General Theory of Molecular Dynamics Simulations

In order to calculate diffusivities of molecules by predicting their movements with time, Molecular Dynamics simulations are used. The simulation basically occurs at three steps called initialization, equilibration and production (Frenkel & Smit, 1996). At the first step, the initial number of particles and their initial positions and velocities are obtained from GCMC simulations and the force on each particle are obtained by computing a simulation that applies Newton's equation of motion. The next step (equilibration) also integrates the same rule and attempts to determine a system that external conditions at steady state and the forces do not cause a flux. Eventually the final step is started where actual simulations are computed with predetermined conditions and predictions of atomic motions through time are settled.

Equation 3.1.5 represents the equations of motion applied in the MD method where r_i is the position vector and F_i are the forces acting on the that particle.

$$m\frac{d^2 r_i}{dt^2} = F_i = (r_1, r_2, r_3, \ldots, r_N), i = 1, 2, 3 \ldots, N \quad (3.1.5)$$

Force is the minus derivative of the potential energy, $U(r_1, r_2, \ldots, r_N)$, with respect to atomic position, as depicted below;

$$F_i(r_1, r_2, r_3, \ldots r_N) = -\nabla r_i \, U(r_1, r_2, r_3, \ldots r_N) \quad (3.1.6)$$

This equation agrees with the conservation of the energy, $E = E_{kin} + U$, where E_{kin} represents the instantaneous kinetic energy. If the external forces are ignored, the total potential energy can be considered as the sum of pairwise interactions between every atom in the system:

$$U = \sum_{i=1}^{N} u(r_{ij}) \quad (3.1.7)$$

where $r_{ij} = r_i - r_j$, $r_{ij} \equiv |r_{ij}|$, and assumes that j >i in order to prevent double counting the interactions.

Finally, overall Force on every particle can be counted as sum of each individual interaction between them and the Equation 3.1.5 becomes;

$$F_j = \sum_{i \neq j}^{N} f_{ij} \quad (3.1.8) \qquad \mathbf{f}_{ij} = - \frac{du(r_{ij})}{d r_{ij}} \cdot \frac{r_{ij}}{r_{ij}} \quad (3.1.9)$$

Newton's third law states that $f_{ji} = -f_{ij}$.

Each atom of every system includes N number of atoms that undergoes a force according to Newton's equation of motion (EOM).

$$F_i = m_i a_i = m_i \frac{d v_i}{dt} = \frac{d p_i}{dt} \quad (3.1.10)$$

While forces acting on a system is conservative meaning depends only on the position of the atoms but not time, force can be derived as potential functions, U (r_1 , r_2 , . . . , r_N) as already described before, see Equation 3.1.6

Combining Newton's EOM with Equation 3.1.6 gives 3.1.11.

$$\frac{d p_i}{dt} = -\frac{dV}{d r_i} \quad (3.1.11)$$

Kinetic energy of an atom can also be calculated by the Newton's rule; hence, Equation 3.1.12 can be transformed to:

$$T_i = \frac{1}{2} m_i v^2{}_i = \frac{1}{2} \frac{m_i^2}{m_i} v^2 = \frac{p_i^2}{2 m_i} \quad (3.1.12)$$

The derivative of the Equation 3.1.13 with respect to momentum gives Equation 3.1.14

$$\frac{d r_i}{dt} = \frac{d T_i}{d p_i} \quad (3.1.13)$$

Equation 3.1.12 and Equation 3.1.13 are called Hamiltonian Equations that provide the time evaluation of coordinates r and momentum p of every atom in the system. These equations can be solved numerically. The solution starts with an assumption that position and velocity of an atom at time t is known. And in order to determine the next position r(t+Δt) and velocity v(t+Δt), Taylor Expansion method can be applied around the known point where Δt is a small time step, i.e. sufficiently small Δt gives more accurate results. The equations 3.1.14 and 3.1.15 describes Taylor expansion of r(t+Δt) and v(t+Δt) where we cut these expansion after second order term.

$$r(t+\delta t) = r(t) + v(t)\,\delta t + \frac{1}{2}\,a(t)\,\delta t^2 + \ldots \quad (3.1.14)$$

$$v(t+\delta t) = v(t) + a(t)\,\delta t + \frac{1}{2}\,b(t)\,\delta t^2 + \ldots (3.1.15)$$

The first order term is v(t) and the second order term gives a(t). When v(t) and a(t) is replaced with the first and second order terms, we achieve Equation 3.1.16;

$$r(t+\Delta t) = r(t) + \Delta t v(t) - \frac{\Delta t^2}{2m}\frac{dV(t)}{dr} \quad (3.1.16)$$

Taylor Expansion can also be applied on velocity formula by taking the derivative of velocity with respect to time and have an equation that determines how to compute a velocity of a particle if the velocity of the previous time is known.

$$v(t+\Delta t) = v(t) - \frac{\Delta t}{2m}\left(\frac{dV(t+\Delta t)}{dr} + \frac{dV(t)}{dr}\right) (3.1.17)$$

It should be noted the the gradient of the previous time and the gradient of the current time must be known for the calculating the velocity of the current time. In summary, the simulation basically proceeds in these steps, respectively:

1. Computes the calculation of the gradient at time t by solving $\frac{dV(t)}{dr}$
2. Next, computes the position of the next time r(t+Δt) using equation 3.1.16
3. Then, it computes gradient of the next time $\frac{dV(t+\Delta t)}{dr}$

4. Finally, the velocity of the next time using equation 3.1.17

As a particle moves, an energy gradient occurs and the MD simulations determine these changes by calculating the position and velocity of particles at each step. Potential energy fluctuates as systems reaches new configurations, thus energy landscape having many local minima points are obtained. These points are crucial for simulating correctly. Therefore adequate sampling of the phase space is required to find all possible minimum energy levels. At each of these samples atoms are at different configurations and every configuration has a probability. The total average probability of the system (<A>) can be determined by carrying out an MD simulation that computes the equation 3.1.9 and 3.1.10 as depicted below.

$$\langle A \rangle = \rho_1 A_1 + \rho_2 A_2 + \rho_3 A_3 + \dots \rho_\infty A_\infty = \int A(q)\rho(q)dq \quad (3.1.18)$$

$$\rho(q) = \frac{e^{-V(q)/kT}}{\int e^{-V(q)/kT} dq} \quad (3.1.19)$$

where A represents the configuration of a system at a particular time and ρ is the probability of that configuration, -V(q) kT stands for potential energy of a particular configuration which is given by Boltzman distribution (k is Boltzman constant, V is volume of the simulation box and T is temperature).

The Classical MD simulation repeats these steps until the end of the simulation which is determined a by cycle number. These calculations provide the next and previous velocities and coordinates of the atoms in the system. The initial coordinates are taken from the literature which come from the experimental studies or predicted by another theoretical studies. Some examples of very well known databases are Cambridge Structural Database (‘Home - The Cambridge Crystallographic Data Centre (CCDC)’, n.d.), Computation-Ready Experimental Meta-Organic Framework (CORE-MOF) Database (Chung et al., 2019) and Protein Data Bank (‘WwPDB: Worldwide Protein Data Bank’, n.d.).

3.2.1. Computing the Energy

Since potential energy is the interaction energy among all particles in the system, it corresponds to gradient. In order to figure out the gradient of a system several terms must be

introduced to the simulation. Force fields are used in MD for calculating the interaction energy. A force field is a combination of formulations that describes the interactions in the system. The interactions occurring within the molecule due to distances, angles, and torsions are called bounded interactions, whereas van der Waals and electrostatic (Coulomb) interactions are called non-bonded interactions.

In Figure 3.1, classical potential types in a system and corresponding formulas are demonstrated. Bonded interactions, which e.g. bond stretching, angle bending, torsion potential and two types of non-bounded potentials, Lennard-Jones and Coulomb potential, are depicted in Figure 3.1. Bond potentials occur within two different atoms which have a linear distance, r_{ij}. Angle bond potentials occur between three atoms with an angular interaction, θ_{ijk}, torsion potential arise between four atoms with a torsion force, θ_{ijkl}. LJ potentials have short range characteristic; however, Coulomb potentials arise between to atoms with long-ranged interaction.

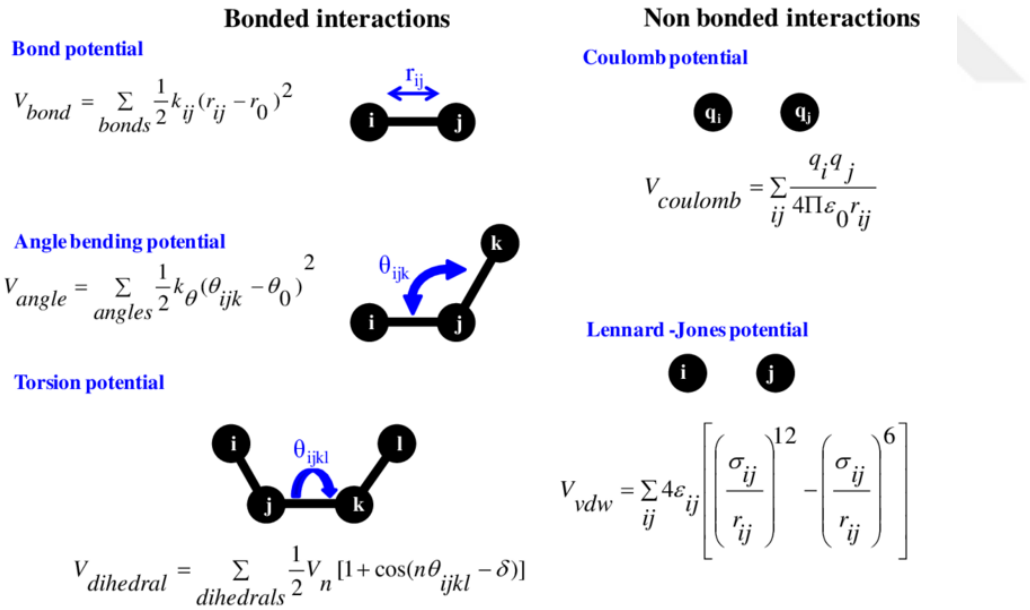

Figure 3.1: Bonded and non-bonded interactions are shown in the figure where k is constant, r_{ij} is the bond distance between two atoms, r_0 is the distance, θ_{ijk} is angle interaction between two atoms, θ_0 equilibrium bond angle (Dantu, 2012).

In order to calculate dispersion type of interactions, Lennard-Jones interactions, ε_{ij} and σ_{ij} are required which are the force field parameters describing energetics and size of the atoms. They are evaluated using Lorentz-Berthelot mixing rules as shown below:

$$\varepsilon_{ij} = \sqrt{\varepsilon i \,.\, \varepsilon j} \quad (3.1.21) \qquad \sigma_{ij} = \frac{\sigma i + \sigma j}{2} \quad (3.1.22)$$

ε and σ are different for each atom and the specific values for each atom can be found at literature.

Force field parameters are specific for each atom type in the system (A. K. Rappe, Casewit, Colwell, Goddard, & Skiff, 1992). The atom type is not just identifies the atomic number but also represents the hybridization state and the local environment of the atom or atoms. There is no 100% correct force field parameter, since they are all calculated using empirical methods. Multiple types of force fields are available in the literature where the parameters they provide is different for each atom (A. K. Rappe et al., 1992). A force field should match several criteria in order to be considered efficient. They must provide the properties of the atom as accurate as possible, must be transferable for variety of structures and properties and must be efficient in computational studies that samples large systems.

3.2.2. Periodic Boundary Conditions

A real macroscopic system includes around 10^{23} atoms in a mole which is impossible to simulate due to tremendous interactions among each other. The simulations usually take into account 10^3 - 10^6 atoms. The Classical Molecular Dynamic uses a simulation box called primary cell that contains the atoms of the system of interest in determined temperature and pressure. Next, MD uses periodic boundary conditions which replicates the primary cell infinite amount of times in three dimension. Then, the simulation computes the potential energies in order to solve equations of motion only for the primary cell that interactions occur only around the nearest cells. The code assumes that any phenomena happening on the primary cell also happens on the other replica cells.

3.2.3. Selection of the cut-off

A cut off function is applied in the simulations in order to limit the calculations of non-bounded interactions. This function has a certain value ensuring that after a certain distance

between two interacting particles, potential energy is not included in the calculations. The cut off distance often has chosen to be 12 – 14 Å which is the most suitable range. In the case of LJ potentials, interaction energies already close to zero between the atoms with a distance greater than 12 Å as in shown in the Figure 3.2 which does not introduce a significant error. However, the coulomb interactions have long-range characteristics which approach to zero very slowly. Hence, after 12 Å distance, the interaction potential can be still significant which could cause discontinuities on the potential gradient and could decrease the reliability of the MD results (Huang, Li, Choi, Nandakumar, & Kostiuk, 2010).

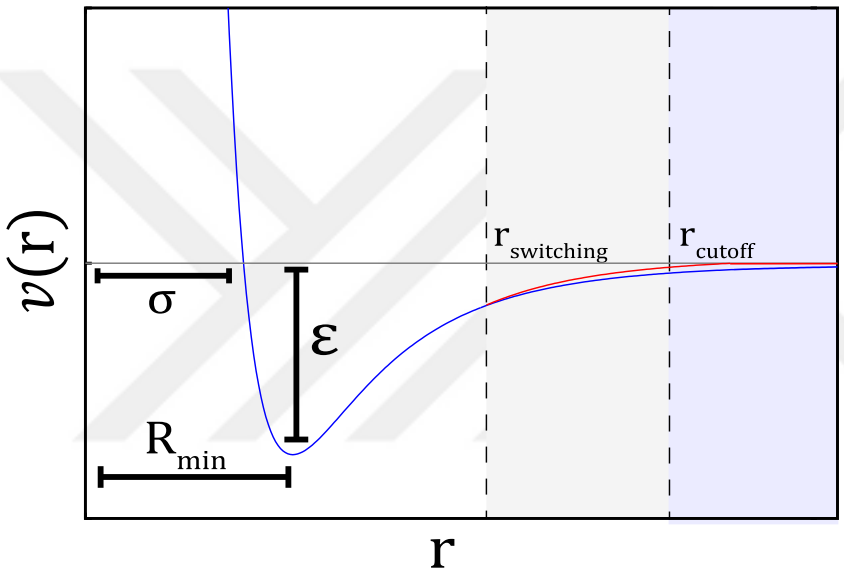

Figure 3.2: Graphical representation of LJ potentials with an interception of a cut-off (r_{cutoff}) where ε is the well depth σ is the distance that makes the intermolecular potential of two particle zero ('LJ-Scheme', 2019).

3.3. Charge Assignment Methods

In this section, a brief information on two charge assignment methods, e.g. Density functional theory (DFT) based Density Derived Electrostatic and Chemical Charges (DDEC) method and Extended Charge Equilibration Method (EQeq) are given.

Density Functional Theory (DFT) is used to solve the Schrödinger equation and obtain information concerning how dense is the charge distribution in that material (Andreoni, 2002).

DFT fits interatomic interactions between numbers of atoms of a many particle system at the ground state by using the summation of the charge density. DDEC theory relies on defining the associated charges of atoms as chemically meaningful and provides electrostatic potential by optimizing the atomic electron density distribution (Manz & Sholl, 2010). As this approach proposed by Manz and Sholl, they trained its performance with several methods including Electrostatic potential fitting methods (ESP) and its extension called REPEAT (Campañá et al., 2009), and with iterative stockholder atom (ISA) (Bultinck, Van Alsenoy, Ayers, & Carbó-Dorca, 2007). According to their results DDEC reproduced accurate, efficient, transferable results for large body of materials.

Calculating atomic charges from quantum-mechanical calculations is very time consuming due to determination of electronic structure. While porous materials have thousands of atoms, this procedure may take hours to finish and therefore increase the cost especially for the studies concerning large body of structures. Various charge equilibration methods have been developed which can reproduce results in minutes and accepted by many researchers. Rappe and Goddard (Anthony K. Rappe & Goddard, 1991) proposed a charge equilibration method (Qeq) in 1991 which uses geometry and experimental atomic properties as basis of the method and uses only the first ionization energies of the atoms. Comparison of atomic charges calculated by Qeq revealed excellent similarities with the experimental observations for simple organic, inorganic, biological, and polymer systems such as H_2O, NH_3, and H_3COH. Furthermore, the method gave reasonable results in simulating porous materials. Yet, Wilmer et. al (Wilmer, Kim, et al., 2012) improved this strategy and added all of the measured ionization energy (first, second, third, etc.) informations into the method called EQeq, and reduced the input parameters from experimental atomic ionization potentials, electron affinities, and atomic radius to a dielectric strength (ε_{eff}, generally 1.67 for low-density materials) and a modified parameter for hydrogen atoms. They used neutral charges for almost all atoms in the structures but changed the “charge centre” of metal atoms to their oxidation states and gave those atoms the same charges at first; Mg: +2, Co: +2, Ni: +2, Cu: +2, Zn: +2 in order to state the partial charges. However this situation makes the method less sensitive. In addition, the method computes atomic charges by assigning the same electronegativity for two

or more atoms that combined in a molecule, which means two different atom types can have the same atomic ionization potential and electron affinity.

EQeq method rewrites the energy of a system by using Taylor expansion rule and makes it a function that relating to the system's charge. As Qeq method, EQeq also constraints the terms after quadratic ones but includes the ionization energies of the electrons. These ionization energies also called the electron affinity, represents the energies of the atoms that gained one electron or lost one. By considering these steps, one can create a new equation that holds the electronegativity and the electron hardness. And while ionization energies of every element in the periodic table up to Z=86 is provided in the literature, a quadratic energy function based on only measured quantities can be obtained. This energy function will include the electronegativity information, hardness and the charges of the atoms that reduced or oxidized up to second order Taylor expansion as shown below:

$$E_A(Q) = E_A(Q^*) + X_{Q^*}(Q - Q^*) + J_{Q^*}\frac{1}{2}(Q - Q^*)^2 \quad (3.1.23)$$

And if this energy function is used to express the total energy of the entire system along with the Coulombic interactions, following equation can be achieved:

$$E_{sys}(Q_1, Q_2, ..., Q_N) = E_{Ak}(Q_k^*) + X_{Q^*}(Q_k - Q_k^*) + \frac{1}{2}J_{Q^*k}(Q_k - Q_k^*)^2 + E_{Ck} + E_{Ok} \quad (3.1.24)$$

E_{ck} represents the interaction energy occurs between the kth atom's charge with all the other atomic charges of the system, and E_{Ok} is the term prevents infinite charge separation between two atoms that brought arbitrarily close together.

In order to assign charges on atoms, EQeq method only runs a simulation that solves equation above by identifying a system with minimum total energy which is not needed to be repeated. It achieves this by using a global dielectric strength ε_r in the calculation of E_{ok}. The only other parameter applied is a representation of unphysical tendency of H atoms. It is ensured that all the H atoms are negatively charged during the assignment of the measured ionization potentials. All the periodic interactions including electrostatic interactions are computed using Ewald summation in the EQeq method. Excellent agreement achieved between EQeq method and various methods including REPEAT (Campañá et al., 2009)(Campañá et al., 2009),

ChelpG (Breneman & Wiberg, 1990) and Qeq (Anthony K. Rappe & Goddard, 1991) which are summarized at Table 3.1. In addition, Wilmer and co-workers simulated carbon capture capacity of 12 MOFs where the atomic charges determined via the same methods (Wilmer, Kim, et al., 2012).

Table 3.1. Average differences of charges of 12 materials calculated by 4 different type of calculation methods (Wilmer, Kim, et al., 2012).

MOF name	**REPEAT**	**ChelpG**	**EQeq**	**Qeq**
HKSUT-1	0	0.05	0.15	0.26
$Pd(2\text{-pymo})_2$	0	0.13	0.24	0.17
IRMOF-1	0	0.02	0.16	0.16
IRMOF-3	0	0.02	0.24	0.23
Zn-MOF-47	0	0.05	0.14	0.24
Ni-MOF-74	0	0.04	0.15	0.15
Co-MOF-74	0	0.04	0.14	0.14
Mg-MOF-74	0	0.05	0.19	0.31
ZIF-8	0	0.07	0.16	0.12
MIL-47	0	0.03	0.11	0.07
UMCM-150	0	0.06	0.11	0.21
UMCM-150(N_2)	0	0.06	0.15	0.29

Figure 3.3 shown below demonstrates CO_2 capture performance of 12 MOFs, whose charges assigned by EQeq and other quantum chemistry derived charges together with neutral framework charges. The figure compares the adsorption results with experimental results where none of the charge scheme matched exactly with itself. Nevertheless, all of the partial atomic charge schemes gave similar predictions for the same process where the CO_2 capture performances using charges calculated by EQeq method gave accurate results than the ones

with Qeq method. The latter, EQeq method needs less computational cost than any other method in that research.

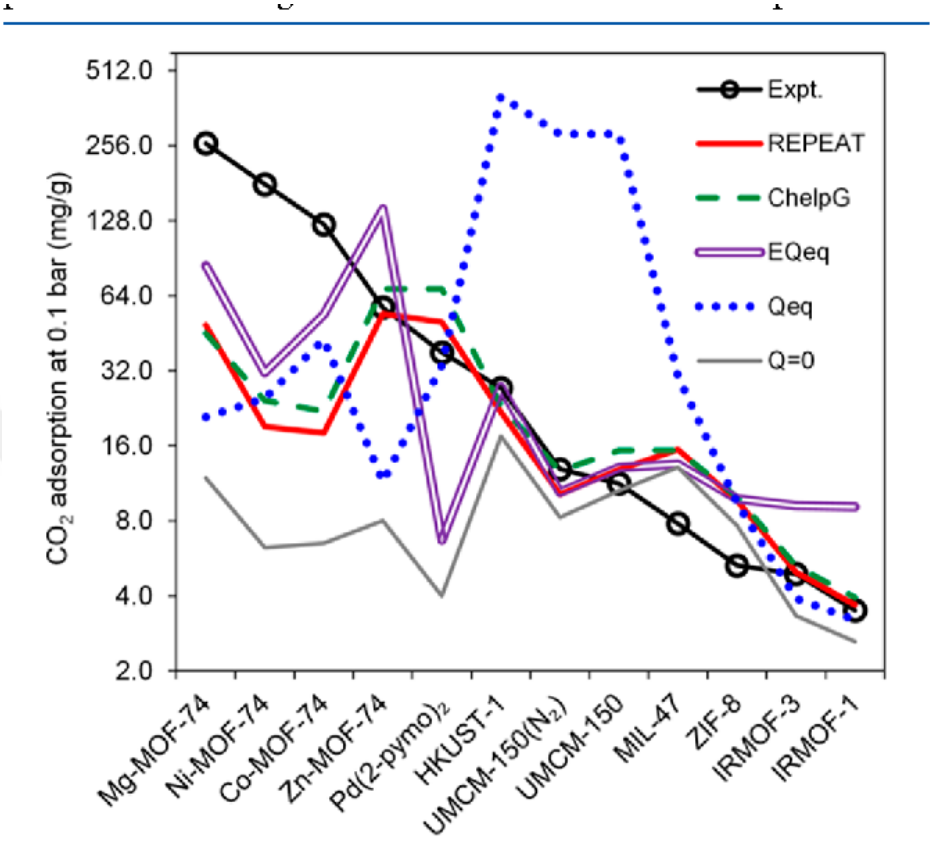

Figure 3.3. Comparison of predicted adsorption amount (mg/g) of 12 MOFs that used five different types of charges with real CO_2 capture experiment results of the same MOFs at 0.1 bar and room temperature (Wilmer, Kim, et al., 2012).

3.4. Prediction Methods for Calculating Permeability and Selectivity of ZIF Membranes

Adsorption based separation performances of the MOFs for binary gas mixtures are predicted using adsorption selectivity parameter which is calculated using the formula shown below:

$$S_{ads(i/j)} = \frac{x_i / x_j}{y_i / y_j} \quad (3.4.1)$$

where x and y are the molar fractions of the adsorbed and bulk phases, respectively.

Permeability and permeation selectivity are the key factors for deciding membrane based separation performances of the ZIFs. The method developed by Sanborn and Snurr (Sanborn

& Snurr, 2001) determines"exact" gas permeabilities calculating Onsager matrix elements and transport diffusivities. From the MD simulations, the Onsager coefficients (L) are calculated using the relation as shown below (Skoulidas et al., 2003).

$$L_{ij} = \frac{1}{d_o V k_B T} \lim_{t \to \infty} \left(\frac{1}{t}\right) \left\langle \sum_{l=1}^{N_l} \left[r_{il}(t) - r_{ij}(0)\right] . \sum_{m=1}^{N_j} \left[r_{jm}(t) - r_{jm}(0)\right] \right\rangle \quad (3.4.2)$$

Here, V is the simulation volume, k_B is the Boltzman constant, and T is the temperature.

In Onsager matrix the diagonal coefficients can be splited into two parts containing self-correlation and cross-correlation contributions. See Ref. (Gurdal & Keskin, 2016) for detailed formulations. Following the determination of the Onsager diffusivities, the Fickian diffusion coefficients are determined by (Skoulidas et al., 2003):

$$D_{ii} = \frac{k_B T}{c_i} \left\langle L_{ii} \left(\frac{\partial \ln f_i}{\partial \ln c_i}\right) T, c_i + L_{ij} \left(\frac{\partial \ln f_j}{\partial \ln c_j}\right) T, c_i \right\rangle \quad (3.4.3)$$

$$D_{ij} = \frac{k_B T}{c_j} \left\langle L_{ii} \left(\frac{\partial \ln f_i}{\partial \ln c_i}\right) T, c_i + L_{ij} \left(\frac{\partial \ln f_j}{\partial \ln c_j}\right) T, c_i \right\rangle \quad (3.4.4)$$

where c_i and c_j are adsorbed loadings of species *i* and j in *i/j* mixture, f_i is the bulk gas fugacity of component *i* when the gas mixture is in equilibrium with an adsorbed mixture with the specified concentrations. Thermodynamic correction factors are formulated as;

$\Gamma_{ij} = \frac{\partial lnfi}{\partial lncj} T, c_{N-j}$ and can be calculated from the mixture isotherms, as explained below.

Mass flux (J) is related with concentration gradient (∇c) and diffusivity (D), as stated by Fick's law shown below:

$$J_i = -\sum_{j=1}^{N} D_{ij} \nabla c_j \quad (3.4.5)$$

Incorporating Onsager and Fickian diffusivity Equations 3.4.2, 3.4.3 and 3.4.4 into the Equation 3.4.6, we can calculate gas flux J_i as follows:

$$J_i = \frac{k_B T}{c_i} \left\langle L_{ii} \left(\frac{\partial \ln f_i}{\partial \ln c_i}\right) T, c_i + L_{ij} \left(\frac{\partial \ln f_j}{\partial \ln c_j}\right) T, c_i \right\rangle \nabla c_j + \frac{k_B T}{c_j} \left\langle L_{ii} \left(\frac{\partial \ln f_i}{\partial \ln c_i}\right) T, c_i + L_{ij} \left(\frac{\partial \ln f_j}{\partial \ln c_j}\right) T, c_i \right\rangle \nabla c_j$$

Mass flux J_i is related to the gas permeability by:

$$P_i = \frac{J_i \varphi}{\Delta f i / l} \quad (3.4.7)$$

where φ is porosity of the ZIF membrane, Δf_i is fugacity difference across the membrane, and l is the membrane thickness. Equation 3.4.8 and 3.4.9 is considered as the formula giving exact results for calculating the gas permeabilities across the nanoporous membrane. This method will be named as detailed method throughout this work. Permeation selectivities are calculated as the ratio of gas permeabilities calculated for binary gas mixtures, as;

$$S_{perm,i/j} = P_i/P_j. \quad (3.4.8)$$

The summarized Sanborn and Snurr method calculates Onsager diffusivities and thermodynamic correction factors for calculating permeability and permeation selectivities. The results are considered as correct answers, however constructing Onsager diffusivity matrix is computationally demanding. Thus, large scale screening of nano porous membranes using detailed method is cumbersome and formulating simplified methods for pre-secreening of membrane performances become inevitable.

The straightforward calculation of gas permeabilities, $P_{app(i)}$, and permeation selectivities, ($S_{perm-app(i/j)}$), have been mostly achieved using an approximate method (Rajamani Krishna & van Baten, 2010). Approximate method is derived from simplification of the detailed method. The gas mixture is assumed 6to be dilute, meaning diagonal elements in the thermodynamic correction factor matrix approach one and off-diagonal ones approach zero. Therefore, one does not have to determine thermodynamic correction factors for calculating permeabilities. Besides, cross correlation contribution of the Onsager diffusivities, between the same species and different species, has been assumed to be negligible due to dilute concentration of species which also eliminates determination of Onsager coefficients for calculating permeabilities and selectivities. As a result, the simplified formulation of the approximate method for permeability and permeation selectivity become as follows:

$$P_{app(i)} = \frac{D_{self,i} c_i \varphi}{f_i} (3.4.9)$$

$$S_{perm\text{-}app(i/j)} = \frac{D_{self,ic_i}}{D_{self,jc_j}} \frac{f_j}{f_i} \quad (3.4.10)$$

Although, approximate method is easy and fast way of screening large number of porous materials, Gurdal and Keskin (Gurdal & Keskin, 2016) reveals that approximate method significantly underestimates the performance metrics with respect to the results obtained using the detailed method. Accordingly, we modify approximate method and propose a new method for predicting membrane performances. Thermodynamic correction factors are still considered in the permeability calculations of the new method, however the cross correlation terms between the same gas species and different gas species are assumed to be negligible. Thus, the new method facilitates results obtained using the approximate method by incorporating thermodynamic correction factors, $\Gamma_{ij} = \frac{\partial \ln f_i}{\partial \ln c_j}\ T, c_{N-j}$ into the equations as shown below:

$$P_{new(i)} = \frac{D_{self,i}\left(\Gamma_{ii} + \Gamma_{ij}\right) c_i \varphi}{f_i} \quad (3.4.11)$$

$$S_{perm\text{-}new(i/j)} = \frac{D_{self,i(\Gamma_{ii}+\Gamma_{ij})c_i}}{D_{self,j(\Gamma_{ji}+\Gamma_{jj})c_i}} \frac{f_i}{f_i} \quad (3.4.12)$$

For detailed derivation of the new method, see Ref. (Gurdal & Keskin, 2016).

Thermodynamic correction factors should be calculated for applying the new method. All calculated adsorbed compositions are then fitted to continuous functions for each component in the $H_2(1)/CH_4(2)$ and $CO_2(1)/H_2(2)$ mixtures as shown below;

$$c_1 = \frac{h_1 f_1}{h_2 f_1 + h_3 f_2 + h_4} + \frac{h_5 f_1}{h_6 f_1 + h_7 f_2 + h_8} \quad (3.4.13)$$

$$c_2 = \frac{s_1 f_2}{s_2 f_1 + s_3 f_2 + s_4} + \frac{s_5 f_1}{s_6 f_1 + s_7 f_2 + s_8} \quad (3.4.14)$$

where h_i and s_i are fitted parameters.

4. RESULTS

This chapter, splitted into two parts, gives all the results and discussions. In the first part, gas permeabilities are calculated using three permeability calculation methods and the results are compared with each other. Our aim is to show which method should be used for accurately capturing gas permeabilities. The second part of the chapter focuses on charge assignment methods. EQeq charge assignment method has been widely used in the literature while carrying out GCMC and MD simulations. We compare the results of EQeq charges with DFT-based DDEC method for several biological MOFs and discuss if EQeq method is sufficiently good for capturing atomic charges calculated by the DDEC method. Our results will be a road map for accurately modelling MOFs and ZIFs.

4.1. Models Used for Permeability Predictions of MOFs Revisited For Binary Gas Mixtures of CO_2, H_2, and CH_4

In this part of the thesis, we use three permeability calculation methods, namely detailed method, approximate approach and new method, in order to determine the CO_2/H_2 and CH_4/H_2 permeation performance of 6 different ZIFs. The detailed method (Sanborn & Snurr, 2001), which gives exact results requires extensive computational time and resources for calculating Onsager coefficient matrix, which is a disadvantage. Thus, using detailed method for calculating permeabilities of large number of MOFs is not feasible. The approximate method proposed by Krishna and Baten (Rajamani Krishna & Baten, 2011) can be considered as a solution of this problem by providing very simple procedure of calculating permeabilities, however studies have shown that this method significantly fails to show good agreement with experimental and computational results. The new method, on the other hand, introduces thermodynamic correction factors into the permeability calculations and gives better predictions for Xe, Kr, and Ar gas mixtures, as shown previously by Gurdal et al. (Gurdal & Keskin, 2016). The new method demands almost the same amount of computational resources as approximate method and makes better predictions. The testing of the new method has been applied only for Xe, Kr, Ar mixtures and its performance for predicting industrially important gas mixtures have not been determined so far. Thus, this thesis will give a valuable input to

the literature by questioning the accuracy of permeability calculation methods carried out for CO_2, CH_4, and H_2 gas mixtures.

4.1.1. Computational Details

In this section detailed computational information for simulations that carried out is provided. In order to simulate adsorption processes of CO_2/H_2 and CH_4/H_2 mixtures via MOFs, GCMC and MD simulations are performed. The feed composition of H_2/CH_4 and CO_2/H_2 mixtures are set as 90/10 and 1/99, respectively, to mimic the composition of syngas mixtures. Calculated adsorption isotherms and self diffusivities of the gas species are used to predict gas permeabilities and permeation selectivities using three approaches: new method, detailed method, and simplified method.

4.1.1.1 ZIF Structures

The permeability models are tested using six ZIF structures, namely ZIF-6, ZIF-10, ZIF-60, ZIF-69, ZIF-79, and ZIF-81. These ZIFs possess different organic linkers, pore sizes, and topologies which enables us to identify the role of structural features on the performance predictions of the new and simplified methods. Properties of the studied ZIFs are summarized in Table 2.

Table 4.2: Structural properties of ZIFs studied in this work including pore limiting diameter (PLD), largest cavity diameter (LCD) (Banerjee et al., 2009, 2008; First & Floudas, 2013; Park et al., 2006).

Material	Composition	PLD/LCD (Å)	Porosity (%)	Topology	Cell Dimensions a,b,c (Å)	Cell Angles (α, β, γ) (deg.)
ZIF-6	$Zn(Im)_2$	6.7/9.5	62.70	GIS	18.52, 18.52, 20.25	90, 90, 90
ZIF10	$Zn(Im)_2$	8.2/12.12	65.00	MER	27.0608, 27.0608,19.406	90, 90, 90
ZIF-60	Zn_2 $(Im)_3$ (mIm)	7.6/12.8	70.82	MER	27.24, 27.24, 19.23	90, 90, 90
ZIF-69	Zn(cbIm)(nIm)	4.9/8.7	57.41	GME	26.08, 26.08, 19.41	90, 90, 120
ZIF-79	Zn(mbIm)(nIm)	4.0/7.5	56.87	GME	25.93, 25.93, 19.65	90, 90, 120
ZIF-81	Zn(bbIm)(nIm)	4.3/8.4	56.65	GME	25.99, 25.99, 19.70	90, 90, 120

Previous X-ray diffraction (XRD) studies are used to identify atomic coordinates of the ZIFs (Banerjee et al., 2009, 2008; Park et al., 2006). Materials are modelled as solvent-free and structural flexibility are neglected throughout our simulations, which can be classified as widely applied simulation strategies for modelling variety of large nano-porous materials (Atci & Keskin, 2012a; Pérez-Pellitero et al., 2010). Pore size can be used to group selected ZIFs. ZIF-6, ZIF-10, and ZIF-60 posses large pores ranging 6.7/9.5 and 7.6/12.8 Å, respectively. The rest of the materials have heterogeneous pore sizes. These ZIFs, namely ZIF-69, ZIF-79, and ZIF-81, have large pores connected through small pore apertures ranging 4.9/8.7, 4.0/7.5, and 4.3/8.4 Å, respectively. One of the common feature of these ZIFs is their large porosities, such as ZIF-60 posses the highest porosity, 70.82 %, followed by ZIF-6 and ZIF-10 ranging as 65 % and 62.70 %, respectively. Considering organic linkers of the ZIFs under consideration, ZIF-6 and ZIF-10 have only imidazolate (Im) type linker with different lengths. ZIF-60, ZIF-69, ZIF-79, and ZIF-81, on the other hand, have hetero-linkers of imidazolate/methyl imidazolate (Im)(mlm), 5-chlorobenzimidazolate/nitro-imidazolate (cbIm)(nIm), methylbenzimidazole/nitro-imidazolate (mbIm)(nIm), and 5-bromobenzimidazolate/nitro-imidazolate (bbIm)(nIm), respectively. ZIF-69, ZIF-79, and ZIF-81 have same topology, GME, however ZIF-10 and ZIF-60 have MER, and ZIF-6 has BCT type topology.

4.1.1.2. Simulation Methodology

Grand canonical Monte Carlo (GCMC) simulations are performed to determine adsorption isotherms of the species in their binary mixtures. Pairwise dispersive interactions are calculated using spherical Lennard Jones 12-6 potential (Verlet, 1967) and mixed interaction parameters are introduced applying Lorentz-Berthelot mixing rules. ZIF atoms are described applying the universal force field (UFF) (A. K. Rappe et al., 1992) parameters which have shown good agreement with the experimental results of gas permeances through ZIFs (Atci & Keskin, 2012a). Besides, comparison of UFF and DREEDING (Mayo, Olafson, & Goddard, 1990) force field parameters give similar results for H_2, CH_4, and CO_2 permeances through ZIF membranes (Atci & Keskin, 2012b). While H_2 and CH_4 molecules are modelled using united atom approach, CO_2 is described as a rigid three-site linear molecule in order to account its quadrupole moment. H_2 is modelled using Buch potential (Buch, 1994), CH_4 and CO_2, on the other hand, are described by TraPPE force field (Martin & Siepmann, 1998). While

electrostatic interactions are neglected for simulations of H_2/CH_4 mixture, partial point charges are defined for each ZIF atom and CO_2 molecule for the simulations of CO_2/H_2 mixture. We apply connectivity-based atom contribution method (CBAC) proposed by Xu and Zhong (Xu & Zhong, 2010). In principle, CBAC method denotes atomic charges by considering corresponding atomic bonding coordination and assumes that framework atoms have identical partial charges if they have same bonding connectivity. Systematic analysis of CBAC method applied on 43 MOFs reveals that CBAC charges, indeed, capture the charges calculated using quantum chemical methods and reproduce experimental adsorption isotherms with good accuracy. Very recently, Lin and co-workers (Changlong Lin et al., 2020) have extended this approach by introducing multilayer connectivity information (m-CBAC), up to 2nd layers with respect to the previous method accounting only the first layer connectivity of a target atom. Comparison of partial atomic charges of 2700 MOFs calculated using m-CBAC and density functional theory based density-derived electrostatic and chemical (DDEC) method reveal a very good agreement. Recently, CBAC method has been applied for modelling n-alkane adsorption on hybrid ZIF-8-90 structures (Sun et al., 2019). Li et al. (L. Li, Wang, Yang, Wang, & Li, 2015) have determined adsorption isotherms of CO_2/CH_4 and CH_4/N_2 on Cu-based flexible MOFs using the CBAC method for charge assignment. GCMC simulations carried out at 298 K are applied for each gas mixture. A cut-off radius of 13 Å is applied for dispersive interactions, whereas electrostatic interactions are truncated at 25 Å. Periodic boundary conditions are always applied in the simulations. A minimum of 3 x 3 x 3 simulation box is used in GCMC simulations and concentration of adsorbed gas molecules are calculated at thermodynamic equilibrium. $3x10^7$ trial configurations in total are performed for each GCMC simulations, where half of the configurations are performed for production. Translation, insertion, deletion and swap of gas particles are applied for each gas species in a GCMC run, and for CO_2 rotational move is applied as well. Self-diffusivities of gas species are calculated applying equilibrium molecular dynamics (MD) simulations in the NVT ensemble (D. C. Rapaport, 2004). MD runs are performed at several feed gas pressure values ranging from 1 bar to 30 bar. The adsorption amounts at corresponding feed gas pressures are taken from the GCMC simulations. Nose-Hoover thermostat algorithm (Evans & Holian, 1985) is used for keeping temperature at 298 K. Each MD run consists of minimum 3 x 3 x 3 unit cell simulation box. MD simulations are performed 16 ns long, and 60 independent MD

trajectories are collected. The mean square displacement of the particles are used to calculate the self-diffusion coefficients ($D_{self,i}$) of the corresponding gas species applying the Einstein relation (Frenkel & Smit, 1996) as depicted below:

$$D_{self,i}=\lim_{t\to\infty}\left(\frac{1}{2d_o t}\right)+\left\langle\frac{1}{N_i}\sum_{l=1}^{N_i}\left[r_{ij}(t)-r_{il}(0)\right]^2\right\rangle \quad (4.1.1)$$

Here, r_{il} (t) stands for the position vector of the ith particle of species i at time t, the angular brackets denote ensemble averages in an equilibrium system, and d_o is the space dimension. The self-diffusivities calculated less than 10^{-8} cm^2/s in any direction of the ZIF membranes are neglected, i.e., no diffusion is considered in that direction.

4.1.2. Comparison of Permeability and Permeation Selectivity of ZIFs Using Three Methods

Permeability and permeation selectivity of several ZIF structures having different pore sizes and topologies are calculated for both CO_2/H_2 and CH_4/H_2 mixtures using the detailed, new, and approximate methods. The results of the detailed method has been considered as the "correct" answers, and the predictions of the new and approximate methods are compared with the results obtained using the detailed method.

Figure 4.4 points the comparison of three methods for the CO_2/H_2 and CH_4/H_2 mixture having 90/10 molar composition, i.e., mixture having 90% mole percent of H_2. There are 60 data points in total for H_2 and CH_4 permeabilities computed at 5 different feed pressures of 6 different ZIF membranes. Permeability predictions of the new and approximate methods are depicted in the y axis using closed and open symbols, respectively. While the results of the detailed method are shown in the x axis, the deviations of the data points from the diagonal line indicate that permeability results calculated using the approximate and/or new methods under predict the correct permeability results. As shown in the Figure 4.4, the new and approximate methods accurately capture the H_2 permeabilities, i.e., the new method gives closer results to the detailed method with respect to the results obtained using the approximate approach. At low feed pressures, we see slight deviations in the calculated H_2 permeability values of ZIF-69, ZIF-79, and ZIF-81 using the approximate approach with respect to the results calculated using detailed method. For instance, at 1 bar, predictions of the approximate

method for H_2 permeability of H_2/CH_4 mixture are 1.62, 1.17, and 1.31 times less than permeability results of the detailed method for ZIF-69, ZIF-79, and ZIF-81, respectively. The predictions of the new method for H_2 permeability of these ZIFs at the same pressure are 1.57, 1.14, and 1.29 times less than the results of the detailed method at 1 bar. As pressure increases, the disagreement between the approximate and detailed methods becomes more significant. For example, at 25 bar feed pressure, approximate approach gives the H_2 permeabilities of ZIF-69, ZIF-79, and ZIF-81 as 2.37, 2.36, and 1.61 times less than the detailed method. The new method, on the other hand, makes better predictions with respect to the approximate method even at higher pressures. The H_2 permeabilities at 25 bar are calculated as 1.51, 1.39, and 1.02 times less than the detailed method calculations for ZIF-69, ZIF-79, and ZIF-81, respectively.

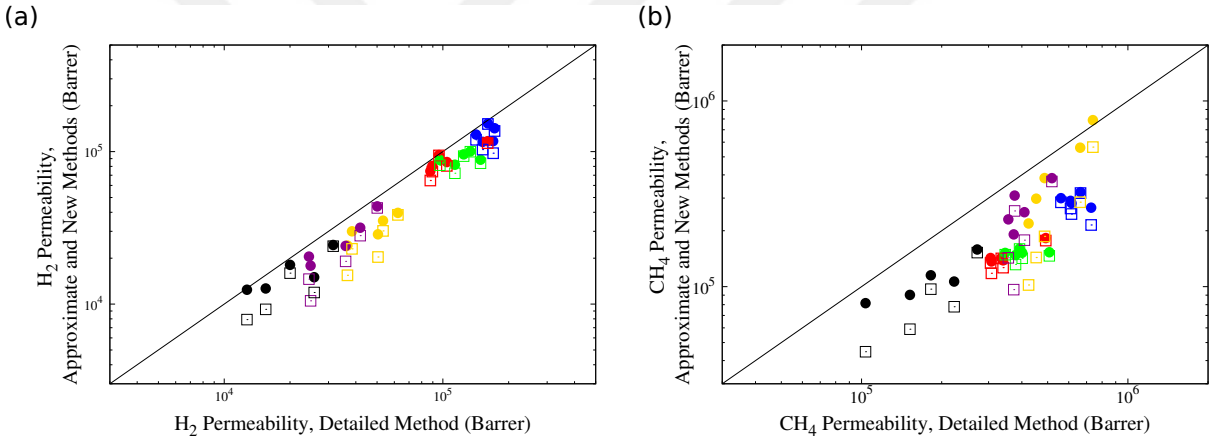

Figure 4.4: Comparison of (a) H_2 permeability (b) CH_4 permeability of ZIF membranes for H_2/CH_4: 90/10 mixture at 298 K and varying feed pressures at 1, 5, 10, 15, and 25 bar. While closed symbols represents values calculated using the new method, open symbols show the results of the approximate approach. Colour code: blue is ZIF-6, red is ZIF-10, green is ZIF-60, yellow is ZIF-69, purple is ZIF-79, and black is for ZIF-81 data.

The permeability results of the new and approximate methods calculated for CH_4 in the H_2/CH_4 mixture show deviations from the detailed method and the deviations become significant especially for the approximate method. Although, we see moderate deviations for ZIF-69, ZIF-79, and ZIF-81 for the calculated H_2 permeabilities, in the case of CH_4 all six ZIFs show large deviations from the values calculated using the detailed method, especially

the approximate method fails to predict the CH_4 permeabilities correctly. For instance, for the ZIF-6, ZIF-10, and ZIF-60 CH_4 permeabilities calculated using the approximate approach are 2.08, 2.36, and 2.46 times less than the permeabilities obtained using the detailed method at 1 bar. As pressure increases, the approximate method points significant deviations from the detailed method, i.e. at 25 bar CH_4 permeabilities are 3.39, 2.60, and 2.88 less than the detailed method permeabilities for the ZIF-6, ZIF-10, and ZIF-60, respectively. The results obtained using the new method, on the other hand, are closer to the"correct" permeability values for all ZIFs under consideration. The new method corrects the permeability predictions of the approximate approach, especially for the ZIF-69, ZIF-79, and ZIF-81. For the remaining ZIFs, ZIF-6, ZIF-10, and ZIF-60, on the other hand, the results of new and approximate methods are close to each other, yet the new method again makes slightly better predictions. For instance, at 25 bars, CH_4 permeabilities calculated using the new method are 2.73, 2.25, and 2.56 times less than the detailed method calculations for the ZIF-6, ZIF-10, and ZIF-60, respectively. In the case of ZIFs having heterogeneous pore size distributions, e.g. ZIF-69, ZIF-79, and ZIF-81, we see even larger deviations between the approximate and detailed methods. At 25 bar, the approximate methods under predicts CH_4 permeabilities by 4.15, 3.87, and 2.32 times with respect to the detailed method for the ZIF-69, ZIF-79, and ZIF-81, respectively. The new method, on the other hand, CH_4 permeabilities are calculated as 1.94, 1.95, and 1.27 for times less than the detailed method for the same ZIFs.

Results suggest that, for the H_2/CH_4 mixture the new method always provide close predictions of the detailed method, at high or low feed pressure conditions, with respect to the approximate method. For the ZIFs having heterogeneous pore size distributions, the results of the approximate method deviate largely from the detailed method for both H_2 and CH_4 permeabilities, especially at high feed pressures. Only for the ZIFs having homogeneous pores size distributions, H_2 permeabilities obtained from the approximate method shows moderate deviations from the detailed method. The new method, on the other hand, always provides better predictions for the H_2/CH_4 permeabilities with respect to the approximate method. Results suggest that as the size of the gas molecules in a binary mixture differs from each other, the approximate method fails to accurately reproduce the permeability of the specie having larger van der Waals diameter, i.e., CH_4 in this case. The deviations of the approximate

approach from the new and detailed methods become pronounce especially for the ZIFs having smaller pores, or large cavities connected through smaller pores. Although, the molar percentage of the CH_4 is not high in the H_2/CH_4 mixture, 10%, larger interaction parameter and larger size of the CH_4 lead to have larger self and cross correlations effect which cannot be captured by the approximate approach.

The CO_2 and H_2 permeability results calculated with the detailed, new, and approximate methods for the CO_2/H_2:1/99 mixture is depicted in Figure 4.5. As a general observation, while the approximate method significantly underestimates the CO_2 permeability of the ZIF membranes under consideration, the new method always gives better predictions. For instance, for ZIF-79 (ZIF-81) CO_2 permeability calculated using the approximate approach at 5 bar and 30 bar are 10.87 (5.24) and 25.77 (6.08) times lower than the results obtained using the detailed method. Using the new method, on the other hand, improves the predictions and the CO_2 permeabilities calculated for ZIF-79 (ZIF-81) at 5 and 30 bar becomes 9.80 (4.77) and 10.80 (3.98) times lower than the results calculated using the detailed method. The large deviations obtained for the CO_2 permeabilities are not only for the ZIFs having heterogeneous pore sizes, but also for the ZIFs having large pores. For instance, for ZIF-10 approximate method and new method gives CO_2 permeabilities by 4.78 and 4.51 times less than the detailed method at 5 bar, and as the pressure increases to 30 bar CO_2 permeabilities become 6.48 and 5.01 times less than the actual results, respectively.

In the case of H_2 permeabilities for the CO_2/H_2:1/99 mixture, on the other hand, both approximate and new methods make better predictions with respect to the CO_2 permeabilities, though the predictions of the new method are again closer to the correct values. For instance, H_2 permeabilities in ZIF-60 (ZIF-69) calculated using the approximate method at 1 and 30 bar are 1.62 (1.07) and 17.48 (2.10) times lower than the actual results. Improved H_2 permeability predictions are obtained using the new method, e.g. for ZIF-60 (ZIF-69) H_2 permeabilities are calculated as 1.08 (0.94) and 0.95 (1.20) times lower than the results obtained using the detailed method at 1 and 30 bar feed gas pressure conditions, respectively. For the ZIFs having large pores, H_2 permeabilities calculated using three methods give similar results at low or high pressures. For instance, at 30 bar H_2 permeabilities in ZIF-10 (ZIF-6) are

calculated 1.48 (1.05) and 1.30 (0.93) times less than the actual values using the approximate and new methods, respectively.

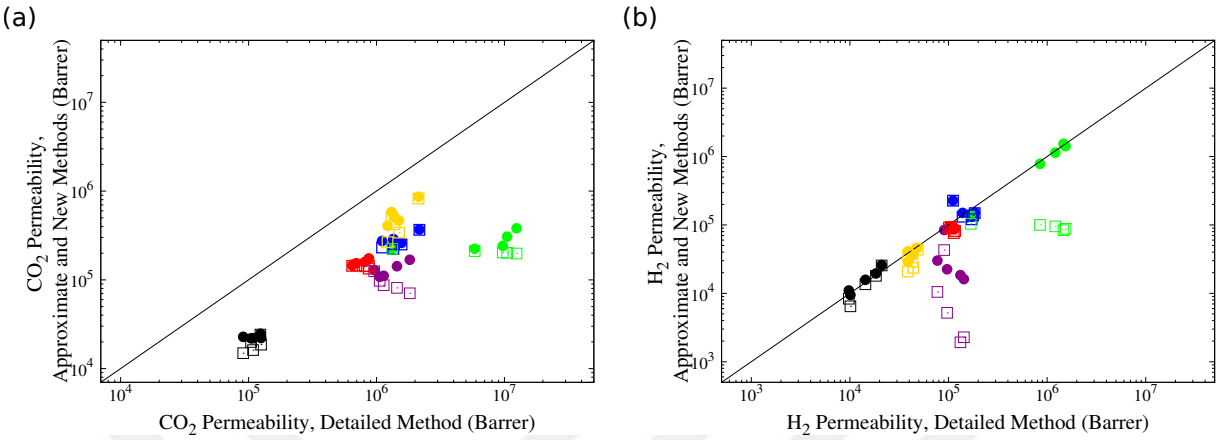

Figure. 4.5: Comparison of (a) CO_2 permeability (b) H_2 permeability of ZIF membranes for CO_2 /H_2: 1/99 mixture at 298 K and varying feed pressures at 1, 5, 10, 20, and 30 bar. While closed symbols represents values calculated using new approach, open symbols show the results of the approximate method. Colour code: blue is for ZIF-6, red is for ZIF-10, green is for ZIF-60, yellow shows ZIF-69, purple shows ZIF-79, and black shows ZIF-81.

As a summary, for the H_2 permeabilities we obtain similar results using the three methods, especially for the ZIFs having large pores. As the pore size distribution of the ZIFs becomes heterogeneous, approximate method results in deviations from the results obtained using the detailed method. New method, on the other hand, always improved the predictions of the approximate method also for the ZIFs having large and small pores or cavities. We see moderate deviations for the CH_4 permeabilities, and the deviations from the detailed method increase with an increase in feed pressure. Introduction of the thermodynamic correction factors in the new method gives better CH_4 permeability predictions than the approximate method. In the case of CO_2/H_2 mixture, we see significant deviations in the CO_2 permeabilities. The new method moderately corrects the predictions of the approximate approach.

While only dispersion type interactions are taken into account for the H_2/CH_4 mixture, electrostatic interactions are also taken into account in the case of CO_2/H_4 mixture. Results suggest that if the gas-ZIF interactions arise only from dispersion interactions, approximate method can make as good predictions as the new method at low pressures. Permeability predictions of the approximate method is also affected by the size of the gas molecule and the

degree of confinement of the gas molecule in the ZIF pores. This explains why the H_2 permeabilities calculated by the approximate method are in good agreement with the detailed method. As the size of the gas molecule increases, as in the case of CH_4, approximate method deviates from the correct results. Thermodynamic correction factors in the new method introduce interactions of the gas-gas pairs as pressure changes and indirectly accounts gas confinement in the ZIF pores, thus, improves the permeability predictions with respect to the approximate approach. As electrostatic interactions play a role in the adsorption process, the results of the approximate and new methods significantly deviates from the results obtained using the detailed method, though the degree of deviation using the approximate method is always larger than the new method.

Figure 4.6-a shows the ratio of CH_4 adsorption to the H_2 adsorption, and the ratio of self diffusion coefficients of H_2 to the self diffusion coefficients of CH_4 at corresponding feed pressures are depicted in Figure 4.6-b. As a general observation, CH_4 is more strongly adsorbed component with respect to the H_2 in ZIFs having relatively small pore sizes, thus we have CH_4/H_2 adsorption ratio greater than one for all the ZIFs under consideration. Pressure averaged adsorption ratios for CH_4/H_2 are calculated as 1.52, 1.23, 1.08, 6.81, 5.75, and 4.43 for ZIF-6, ZIF-10, ZIF-60, ZIF-69, ZIF-79, and ZIF-81, respectively. For the ZIFs having large pores, e.g. ZIF-6, ZIF-10, and ZIF-60, the adsorption amounts of CH_4 and H_2 are comparable. For the ZIFs having relatively small pore sizes, ZIF-69, ZIF-79, and ZIF-81, the CH_4 adsorption significantly dominates H_2 uptake. The adsorption loading ratio is almost constant with increasing feed pressure for all the ZIFs, except for ZIF-69. For ZIF-69, we see an increase in the H_2 uptake with respect to the CH_4 as pressure increases, thus a sharp decrease is observed in the CH_4/H_2 adsorption ratio.

For all the ZIFs, the more mobile component becomes H_2 yielding large self diffusivity ratios of H_2/CH_4 as a function of feed pressure, see Figure 4.6-b. We see a slight decrease in the H_2/CH_4 self diffusion ratio for all the ZIFs as pressure increases. The pressure averaged self diffusivity ratios for H_2/CH_4 are calculated as 6.24, 6.70, 5.74, 6.48, 5.63, and 6.43 for ZIF-6, ZIF-10, ZIF-60, ZIF-69, ZIF-79, and ZIF-81, respectively. While adsorption loading ratios of the ZIFs differ from each other with respect to their pore size distributions, pressure averaged

ratio of self diffusivities are similar for all the ZIFs under consideration. According to the permeability calculations, permeability of the significantly fast moving component, H_2, has been calculated similarly by the new and approximate methods which are close to the values calculated using the detailed method. For the component diffusing significantly slower, CH_4, the significant deviations have been observed between the approximate and the detailed method, where the new method makes better predictions. Results suggest that predictions of the new and approximate methods are affected by the the ratio of self diffusivities rather than the ratio of adsorption loadings.

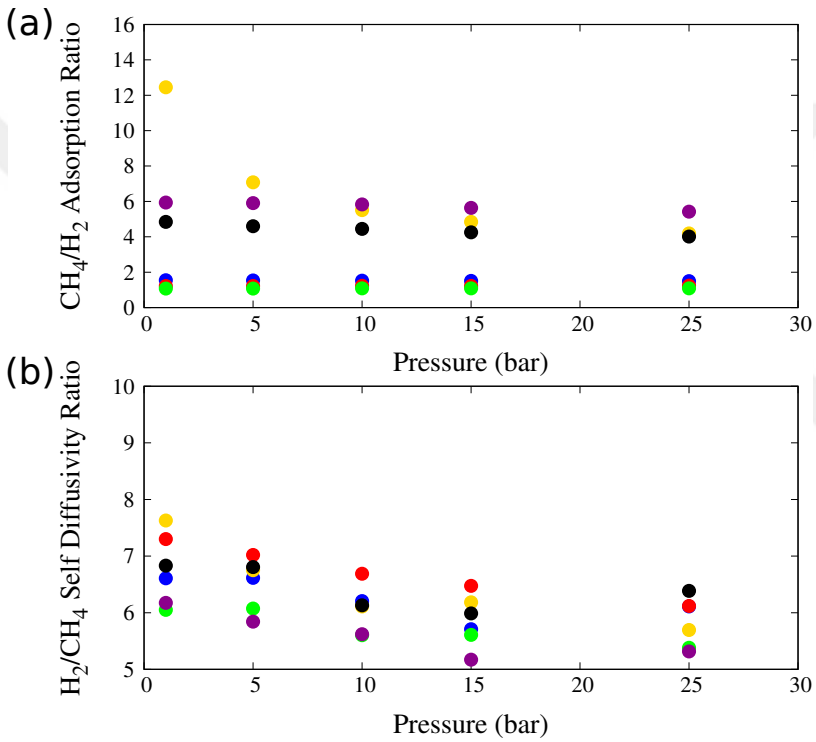

Figure. 4.6: Comparison of (a) CH_4/H_2 adsorption ratio and (b) the ratio of self diffusivities for H_2/CH_4 as a function of feed pressure. Color code: blue is for ZIF-6, red is for ZIF-10, green is for ZIF-60, yellow shows ZIF-69, purple shows ZIF-79, and black shows ZIF-81.

The shed lighter on the reasons of deviations between three methods, the Onsager coefficients which relate forces to fluxes are analysed. While diagonal Onsager coefficients for H_2 (L_{11}) and CH_4 (L_{22}) are plotted in Figure 4.7-a. Off-diagonal, L_{12}, and the diagonal terms for H_2 (L_{11}) and CH_4 (L_{22}) are compared in Figure 4.7-b and 4.7-c, respectively. If the linear cross coefficients are assumed to be symmetric, then the off-diagonal terms are accepted to be equal to each other by the Onsager formalism of diffusion (Zielinski & Alsoy, 2001), i.e. $L_{12}=L_{21}$.

Calculated L_{11} and L_{22} values are similar to each other for ZIF-69, ZIF-79, and ZIF-81, whereas for the large pored ZIFs L_{11} is larger than the L_{22}. Results suggest that for the ZIFs having relatively large pore sizes, ZIF-6, ZIF-10, and ZIF-60, the self-correlation effects for H_2 is larger than the self correlation effects for CH_4 during the diffusion process. The reason is attributed to the comparable adsorption amount of H_2 with respect to the CH_4 in ZIFs having large pores. For the other ZIFs, instead, H_2 is dilute in the adsorbed phase, thus self-correlation effects are not as significant as the aforementioned case. The cross correlation effects, L_{12}, are compared with L_{11} in Figure 4.7-b and results show that the self-correlational effects for H_2 are larger than the cross correlation effects for H_2 and CH_4, especially for the ZIF-6, ZIF-10, and ZIF-60.

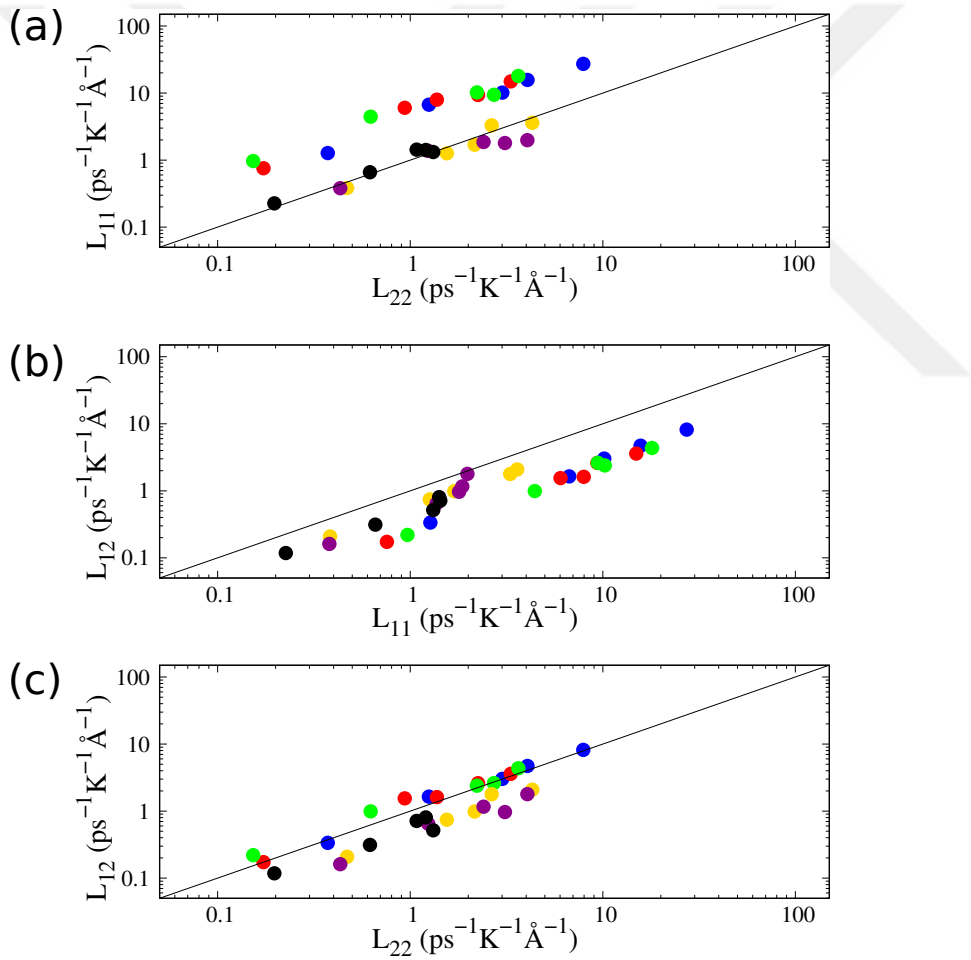

Figure. 4.7: Comparison of the diagonal Onsager coefficients of H_2 (1) and CH_4 (2), the off-diagonal and diagonal Onsager coefficients of (b) H_2(1) and (c) CH_4(2) at 298 K and varying feed pressures at 1, 5, 10, 15, and 25 bar sorted top to bottom respectively. Color code: blue is for ZIF-6, red is for ZIF-10, green is for ZIF-60, yellow shows ZIF-69, purple shows ZIF-79, and black shows ZIF-81.

This implies that, as the self diffusivity of H_2 is significantly larger than the self diffusivity of CH_4 for all the ZIFs, H_2 diffusion is dominantly affected by the other H_2 molecules, rather than CH_4 component, during the diffusion process. The self correlation effects for CH_4, on the other hand, are comparable with the cross correlation effects for CH_4 and H_2, see Figure 4.7-c According to the results, CH_4 permeability predictions of the approximate method deviates significantly from the results of the detailed method shown in Figure 4.4, which can be attributed to the slower diffusion of CH_4 as well as similar self and cross correlations effects for CH_4. These effects are not taken into consideration in the formulation of the approximate method, however inclusion of the thermodynamic correction factors in the new method corrects the predictions of the approximate approach.

The significant deviations of the approximate and new methods from the detailed method, especially for the CO_2, in CO_2/H_2 mixture are investigated by the same analysis and comparisons are carried out before. Figure 4.8 compares CO_2/H_2 adsorption ratio and H_2/CO_2 self diffusivity ratio, respectively. As a different trend observed for the H_2/CH_4, while ZIF-69, ZIF-79, and ZIF-81 show larger affinity for the CO_2, the rest of the ZIFs under consideration favour H_2 adsorption over CO_2. The pressure averaged CO_2/H_2 adsorption ratios are calculated as 0.35, 0.28, 0.32, 5.41, 10.70, and 2.51 for ZIF-6, ZIF-10, ZIF-60, ZIF-69, ZIF-79, and ZIF-81, respectively. The largest CO_2/H_2 adsorption ratio is observed for ZIF-79. Self diffusivity ratios calculated for the H_2/CO_2 mixture are significantly larger than the ratios calculated for the H_2/CH_4 mixture. The pressure averaged CO_2/H_2 self diffusivity ratios are calculated as 18.92, 16.63, 14.35, 34.52, 60.0, and 185.13 for ZIF-6, ZIF-10, ZIF-60, ZIF-69, ZIF-79, and ZIF-81, respectively. H_2 is fast moving component with respect to CO_2, and we observe significant self diffusion rate of H_2 with respect to CO_2 especially for the ZIFs having small pore sizes as can be seen in the adsorption rates of ZIF-69, ZIF-79, and ZIF-81.

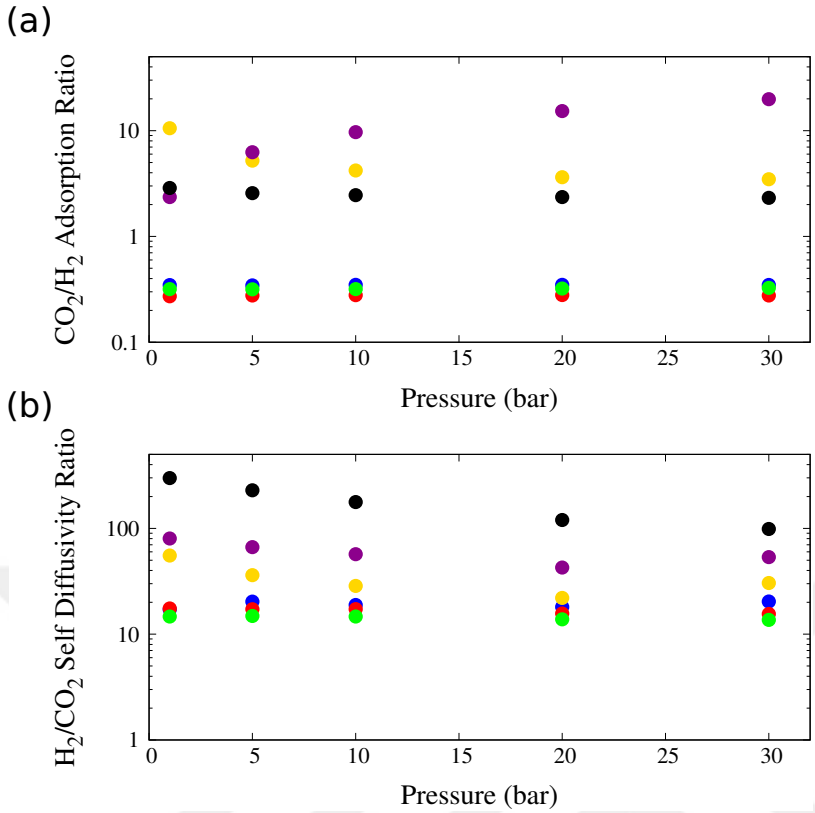

Figure 4.8: Comparison of (a) CO_2/H_2 adsorption ratio, plotted in log scale, and (b) the ratio of self diffusivities for H_2/CO_2 as a function of feed pressure. Color code: blue is for ZIF-6, red is for ZIF-10, green is for ZIF-60, yellow shows ZIF-69, purple shows ZIF-79, and black shows ZIF-81.

The diagonal and off-diagonal Onsager coefficients for CO_2 (1) and H_2 (2) are compared in Figure 4.9. As it is shown in Figure 4.9-a, self correlation effects for H_2 are larger with respect to the self correlation effects for CO_2. While self and cross correlation effects for CO_2 are similar to each other in ZIF-69, the cross correlation effects for CO_2 are larger than correlation effects between CO_2 molecules for the rest of the ZIFs under consideration, see Figure 4.9-b. On the contrary, self correlation effects between H_2 molecules are larger than the cross correlation effects for H_2 for all the ZIFs. Since H_2 is the significantly fast diffusing component, self correlation effects for H_2 dominates self correlation effects for CO_2. Besides, cross correlation effects between H_2 and CO_2 dominate self correlation effects for CO_2.

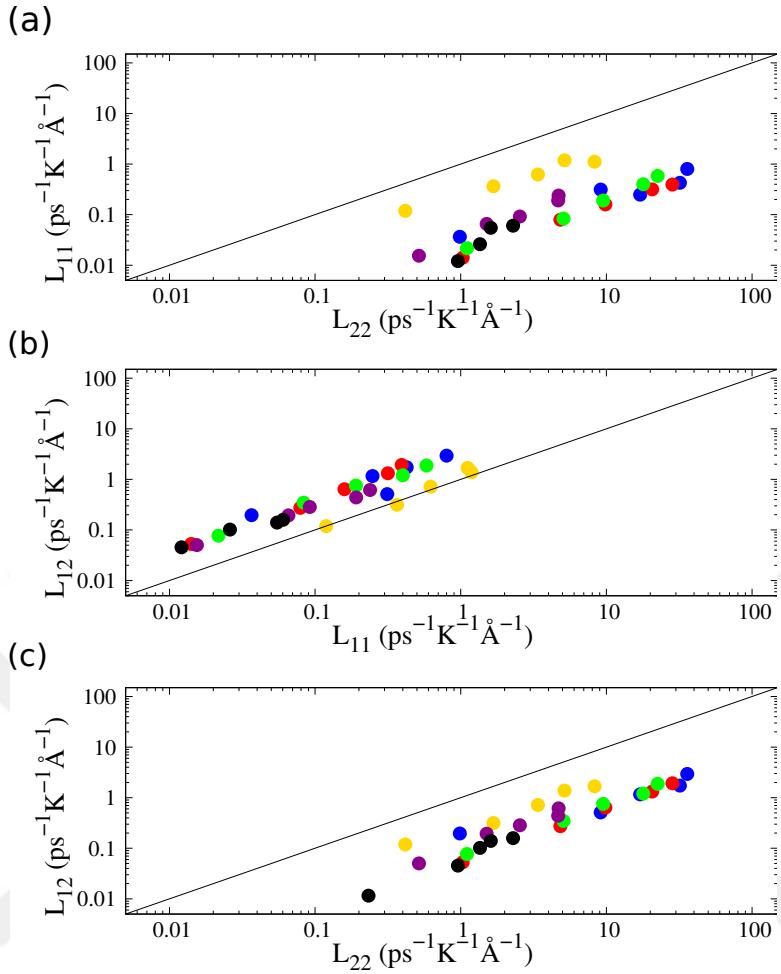

Figure. 4.9: Comparison of (a) the diagonal Onsager coefficients of CO_2 (1) and H_2 (2) and the off-diagonal and diagonal Onsager coefficients of (c) CO_2 (1) and (d) H_2 (2) at 298 K and varying feed pressures at 1, 5, 10, 20, and 30 bar. Color code: blue is for ZIF-6, red is for ZIF-10, green is for ZIF-60, yellow shows ZIF-69, purple shows ZIF-79, and black shows ZIF-81.

We observe the largest deviation between approximate and detailed method for CO_2/H_2 mixture for ZIF-60 and ZIF-79, see Figure 4.5. At 30 bar, CO_2 permeability for ZIF-60 calculated by the approximate method deviates from the detailed method by 62.78 times. As the same vein, H_2 permeability for ZIF-60 deviates from the detailed method by 17.48 times using the approximate method. For ZIF-79, $CO_2(H_2)$ permeability at 30 bar deviates from the detailed method by 25.77 (68.70) times using the approximate method. Results suggest that the mispredictions of the approximate method can not be only explained by the pore size distributions, since pore size of ZIF-60 is larger than ZIF-79, however we observe large deviations for both ZIF-60 and ZIF-79. From Figure 4.9, we obtain large H_2 adsorption over CO_2 for ZIF-60, thus H_2 diffusion rate in ZIF-60 pores becomes lower. For the CO_2, on the

other hand, we obtain large CO_2 uptake with respect to H_2 for ZIF-79 in which CO_2 diffusion becomes significantly slow. In the case of H_2/CH_4 mixture, though, we do not observe very large CH_4/H_2 adsorption ratios or H_2/CH_4 diffusion ratios as in the case of CO_2/H_2 mixture. The same argument also holds for comparison of the Onsager coefficients. While the ratio of pressure averaged ratio of diagonal Onsager terms of $H_2(2)/CO_2(1)$ (L_{22}/L_{11}) is around 50 for ZIF-60, it is around 5 for the $H_2(1)/CH_4(2)$ (L_{11}/L_{22}). In the case of ZIF-79, while pressure averaged ratio of L_{22}/L_{11} for $H_2(2)/CO_2$ (1) is calculated as 25, the same ratio for $H_2(1)/CH_4(2)$ is calculated as 1.5. The same trend also holds in the case of ratio of diagonal and off-diagonal coefficients, where $H_2(2)/CO_2(1)$ mixture has larger ratio then the $H_2(1)/CH_4(2)$ for both ZIF-60 and ZIF-79. Results suggest that, by comparison to the H_2/CO_2 mixture H_2/CH_4 mixture behaves as having similar components even though size and interaction parameters of H 2 is different than CH_4. The common feature in the simulations is that both H_2 and CH_4 are interacting with the ZIFs only through LJ potential.

In the case of H_2/CO_2 mixture, though, electrostatic interactions are taken into account for CO_2 in addition to the LJ type interactions. Thus, H_2 and CO_2 are interacting differently with the pores and behaving as different components leading significant deviations in permeabilities calculated by the approximate method. Inclusion of the thermodynamic correction factors in the new method slightly corrects the predictions of the approximate method for the CO_2/H_2 mixture.

Figure 4.10 compare the CH_4 and CO_2 permeation selectivities for their binary mixtures with H_2. As it can be seen from Equation 3.4.8 and 3.4.12, the ratio of thermodynamic correction factors creates the only difference between the permeation selectivity formulations of the approximate and new methods. If this ratio is close to 1, then permeation selectivity calculated by the approximate and new methods should be the same. CH_4 permeation selectivities calculated by the new and approximate methods are agree well with the detailed method, see Figure 4.10-a. For CO_2 permeation selectivity, on the other hand, both new and approximate method fail to predict the results obtained by the detailed method.

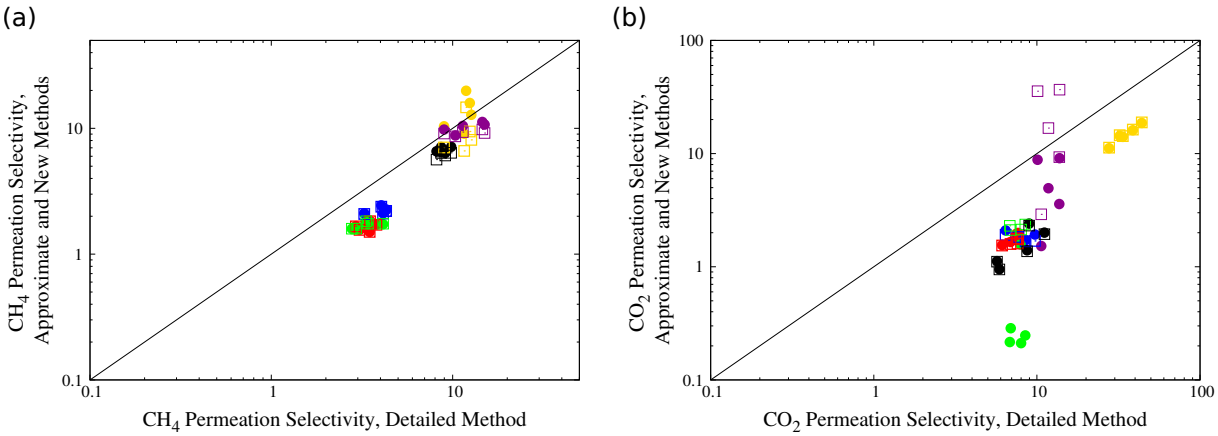

Figure. 4.10: (a) Permeation selectivity of ZIF membranes for H_2/CH_4 mixture at 298 K and varying feed pressures at 1, 5, 10, 15, and 25 bar. (b) Permeation selectivity of ZIF membranes for CO_2/H_2 mixture at 298 K and varying feed pressures at 1, 5, 10, 20, and 30 bar. Color code: blue is for ZIF-6, red is for ZIF-10, green is for ZIF-60, yellow shows ZIF-69, purple shows ZIF-79, and black shows ZIF-81.

4.2. The Accuracy of Charge Assignment Methods: A Case Study For Bio-MOFs

Biological Metal Organic Frameworks (Bio-MOFs) are a class of MOFs which consists of amino acids, sugar or nucleobases as an organic linker with biocompatible metal cations (Cai, Huang, & Li, 2019). They have been employed in many applications owing to their harmless affect on environment and human body and they are non-toxic materials with regular large porosity and chemical functionality (Cai et al., 2019).

Studies have shown that Bio-MOFs can be treated to separate, store and deliver cationic drug molecules as well as gas molecules owing to their ease of changing pore size, flexibility and interconnectivity (Erucar & Keskin, 2015; Verma, Mishra, & Kumar, 2010). While these materials are great candidates as a membrane and adsorbent structures, proper understanding the properties, abilities and comparison of Bio-MOFs with other porous materials is crucial in order to design and develop better Bio-MOFs. Pre-screening of Bio-MOFs using computational studies have been used more and more recently. Molecular simulations are an efficient and fastest way to sort the most promising materials among thousands of them, hence lead the way for experimental studies. In this concept, charge assignment of atoms is a critical step to depict the promising Bio-MOFs characteristic, thus tend to create more valid and fast molecular simulations. And finally point the researchers to use more realistic computational

simulations that pave the way of developing the most promising materials mainly for the experimental gas adsorption processes and medical practices.
Even small chemical difference between Bio-MOFs, may change the computing procedure of the method, thus, MOFs with unique atom types or number of atoms would have different charges from each other.

4.2.1. Computational Details

Using the atomic charge density information obtained by Density functional theory (DFT), we perform a simulation applying DDEC method to assign the net atomic charges of several Bio-MOFs (Andreoni, 2002; Limas & Manz, 2018). EQeq method is also used to calculate atomic charges of the same MOFs (Wilmer, et al., 2012). Both calculations are performed by using electronic structure and MD software package CP2K (Kühne et al., 2020). CP2K can perform atomistic simulations of solid, molecular, material and biological systems by creating general framework for Molecular Dynamics, Monte Carlo, and DFT calculations(Kühne et al., 2020).

Density functional theory is a successful and widely used theorem used to specify electronic structure which can help to understand chemical structure and reactiveness of that particle (Baseden & Tye, 2014). It applies fundamentals of quantum mechanics for treatment of electron−electron interactions in systems with small and large systems of atoms, molecules or solids. It uses a normalized wave function and electron density computation in order to find total energy of the system with electronic interactions. DFT does not need experimental input parameters. Among all electronic structure theories, DFT is concluded as the most cost efficient theory for large molecules with a high accuracyb(Baseden & Tye, 2014). Electronic charge density of the atoms for each BiO-MOF is determined by DFT which Is then used for the DDEC charge calculations.

Crystallographic data of the considered biological MOFs are taken from CoRE-MOF Database where crystal structures, pore analytics, and physical property of over 14.000 porous MOFs are stored (Chung et al., 2019). Since the databases that contain the coordinates of solvent or ligand molecules additionally in the crystallographic data of MOFs, we used

modified version of the Bio-MOFs from the updated version of the same database published in 2019 in order to enhance accuracy.

DDEC net atomic charges of the considered MOFs are computed using CP2K simulation package. In every CP2K simulation molecularly optimized Basis Sets and Pseudo-potentials are assigned for each atom. Basis sets provides the informations such as contraction coefficients, principle quantum number, minimum and maximum angular momentum quantum number, number of Gaussian exponents of an atom. In addition, only the number of valence electrons in the Bio-MOF atoms have been taken into consideration explicitly.

Table 4.3 collects the data for biological MOFs which is used for the training atomic charges calculated by the EQeq method reference to the DDEC based charges with additional datas including the metal atom ratio of the framework that added for the efficient comparison.

Table 4.3. Considered Bio-MOFs in the study with data of their name, ligand, metal sites, LCD/PLD (Å), density (g/cm^3), void fraction, surface area (SA) (m^2/g), total number of atoms and the ratio of metal atoms respect to total number of atoms (Atci et al., 2011).

Bio-MOF	**Ligand**	**Metal Sites**	**LCD/PLD (Å)**	**Density (g/cm^3)**	**Void Faction**	**SA (m^2/g)**	**Total Atoms**	**Metal Ratio**
AGOFEJ	Formamide	Cu,N	12.61/8.72	0.58	0.76	3269.05	904	37.6
BELTUJ	Formamide	Co,P	5.65/4.19	1.09	0.51	970.49	680	28
ADASOP	Formamide	Zn	18.04/6.69	0.63	0.84	3346.21	552	23
ADUWIH	Formamide	Zn	9.28/6.55	0.72	0.72	2605.83	444	37
EZOFEF	Formamide	Ni	11.24/4.57	1.02	0.64	1161.91	288	14.25
LONWIW	Formamide	Mg	6.33/5.31	0.83	0.66	2526.00	228	19
ADUWON	Formamide	Ni	16.38/6.00	0.52	0.8	4298.28	208	11
ACIBOE	Formamide	Zn	8.26/7.03	1.1	0.63	1609.46	160	13.3

4.2.3. Comparison of Charge Assignment Methods

C, O and H atomic charges of 8 Bio-MOFs that are calculated using DDEC and EQeq approaches are given in Figure 4.12, 4.13 and 4.14, respectively. These figures give an insight to the comparison of EQeq charges with respect to the DDEC charges. As DDEC method is based on Density Functional Theory (DFT), it assumed to reproduce “accurate” charges while EQeq method relies on approximations. EQeq applies neutral charges for all atoms except for metal cations where oxidation states are assumed as “charge centres” while calculating the point charges. This assumption causes to assign same charges to the atoms without considering their chemical environment which in principle could affect the charge of the atom and lead to deviation from real charges.

In Figure 4.12, charges of each C atoms of Bio-MOFs assigned by DDEC and EQeq method is depicted in x-axis and y-axis, respectively. If all points representing atomic charges of the Bio-MOFs are collapsed on the dashed line (diagonal) it means EQeq and DDEC has an excellent agreement, on the contrary, any mismatches mean deviations of EQeq from the DDEC method. Figure 4.12 indicated that EQeq results deviate significantly from the results calculated using the DDEC method. As a general observation, C charges are calculated very similar with each other using the EQeq method. However, these charges are assigned differently by the DDEC mehtod. For instance, for the BELTUJ the charge of the one of the C atom is calculated as -0.5 with the DDEC method, however it is determined as 0.029 with the EQeq. For the ADUWIH, the C atom charge is calculated almost +1 with DDEC, however it is assigned as 0.03 with EQeq. Thus, EQeq shows significant failure in calculating the charges of the C atoms in the considered Bio-MOF structures.

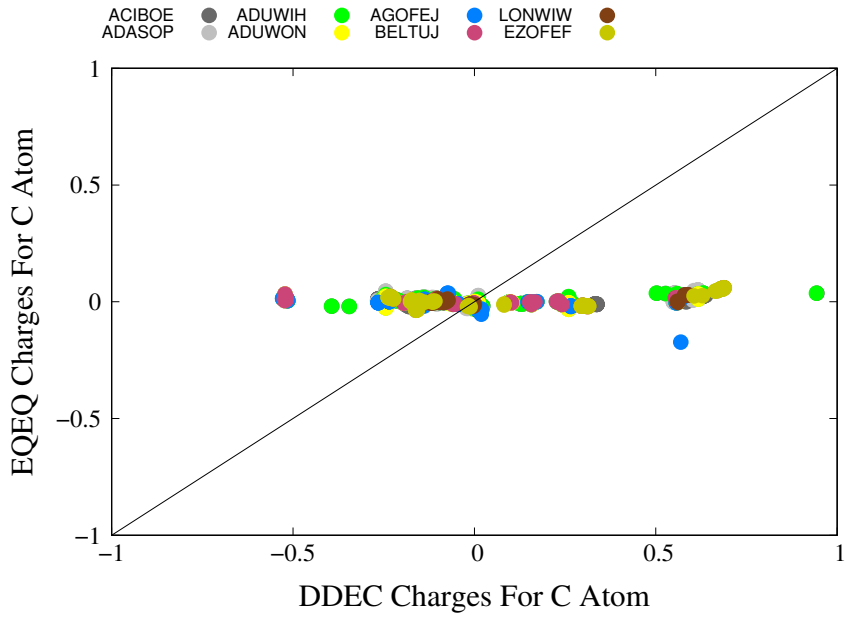

Figure 4.11. Comparison of atomic charges of Carbon (C) atoms in the considered Bio-MOFs computed by EQeq and DDEC methods.

The study reported by Ongari and co-workers says that any bond between C and N, EQeq method tends to deviate with respect to the DDEC charges (Ongari et al., 2019). AGOFEJ consisting of many C atoms with 56 N atoms and being the largest MOF among 6 other described in this work, has again large deviations for the charges of the C atoms.

In Figure 4.13, the case for O atoms are shown. Calculated point charges of every O atom in 8 Bio-MOFs is compared with each other in the figure. As a general observation, O charges are calculated by the EQeq are overestimated with respect to the DDEC charges. The DDEC charges are based on DFT calculations that takes into account the electron density, hence considered to give correct charges, any discrepancies between EQeq and DDEC charges can be considered as the deviations from the real charges. Figure 4.13 demonstrates that there is a signifiant inequality among the atomic charges of the Bio-MOFs calculated by DDEC and EQeq approaches. One of the most noticeable deviation can be seen for EZOFEF, where the charges of the first three O atoms in the crystal structure of the Bio-MOF are calculated as -0.173, -0.15 and 0.138 by the EQeq method, while the DDEC method calculated the same

Oxygen atom charges as 0.549, 0.526 and 0.516 which are significantly far from each other (~0.376 for each). This difference may cause from the calculation strategy of the charge assignment methods where EQeq considers just the ionization energies of the atoms with only atomic positions of the framework and not regarding quantum mechanical properties. In addition, these deviations are expected due to the nature of the EQeq method accepting the same electron affinity for all the Oxygen atoms. This assumption can lead discrepancies where there are many Oxygen atoms in different locations of the framework with different electronegativity and different interaction potentials with the surrounding atoms. Similarly, the number of metal atoms in the structure could affect the electronegativity of the other atoms. Oxygen atom charges calculated by the EQeq method deviates for ADUWIH, AGOFEJ and BELTUJ with respect to the DDEC charges where ADUWON and ACIBOE have less metallic center as wil be explained later.

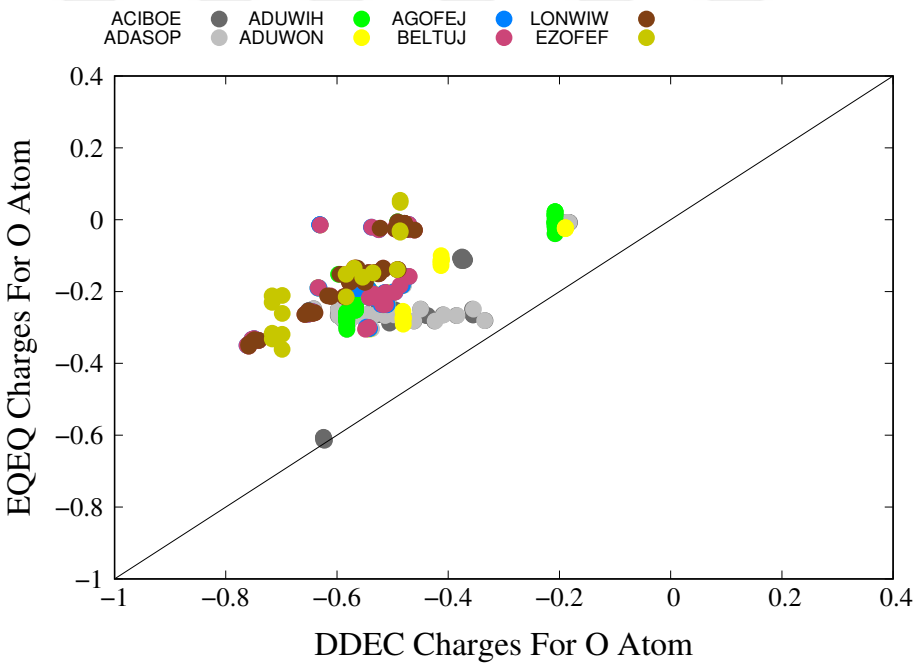

Figure 4.12. The atomic O charges of Bio-MOFs of interest calculated by EQeq method compared with with the charges calculated by DDEC method.

LONWIW and EZOFEF show the highest difference between the EQeq and DDEC charges. The reason may be the fact that EQeq charges assign the same charge (+2) for Ni and Mg atoms at the initial state which makes the method less sensitive considering that every Mg

atom of LONWIW has 6 Oxygen bond and EZOFEF has 16 Ni atoms having 4 O bond each. These bonds create electrostatic interaction potentials due to ionic character of the bonds. The EQeq method uses Ewald summation to calculate these kinds of electrostatic charges where DDEC uses electron density approaches to obtain electrostatic potential, therefore, EQeq charges are expected to give less accurate results with the Bio-MOFs having this kind of interactions.

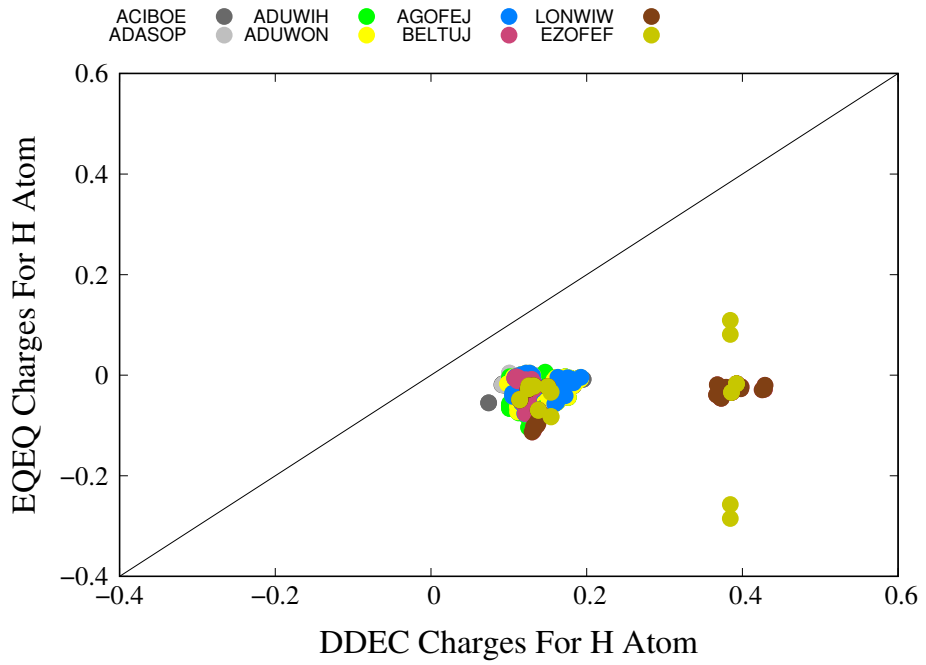

Figure 4.13. Comparison of H atom charges of Bio-MOFs computed by EQeq method with respect to DDEC based calculated charges.

In the case of H atoms, the EQeq charges again fail to accurately capture the charges calculated using the DDEC method. Almost all of the H atom charges of the Bio-MOFs were similar to each other which can be seen the clustered area in the Figure 4.14 apart from LONWIW and EZOFEF where slight deviations arose. H atoms become H – ions when they gain an electron which is more stable than H atom with one electron which is not considered by the EQeq method. The EQeq method uses a dielectric strength and a modified parameter in order to avoid non-physical partial charges assigned to the H atoms. This correction is aimed to enhance the accuracy of the EQeq method reference to the DDEC charges. However, the results are not promising, especially for LONWIW and EZOFEF. Ongari and co-workers

indicated that the large number of H atoms in the internal surfaces of the structures leads to instabilities for the EQeq method owing to large number of fitting parameter calculations leading to high degree of error (Ongari et al., 2019).

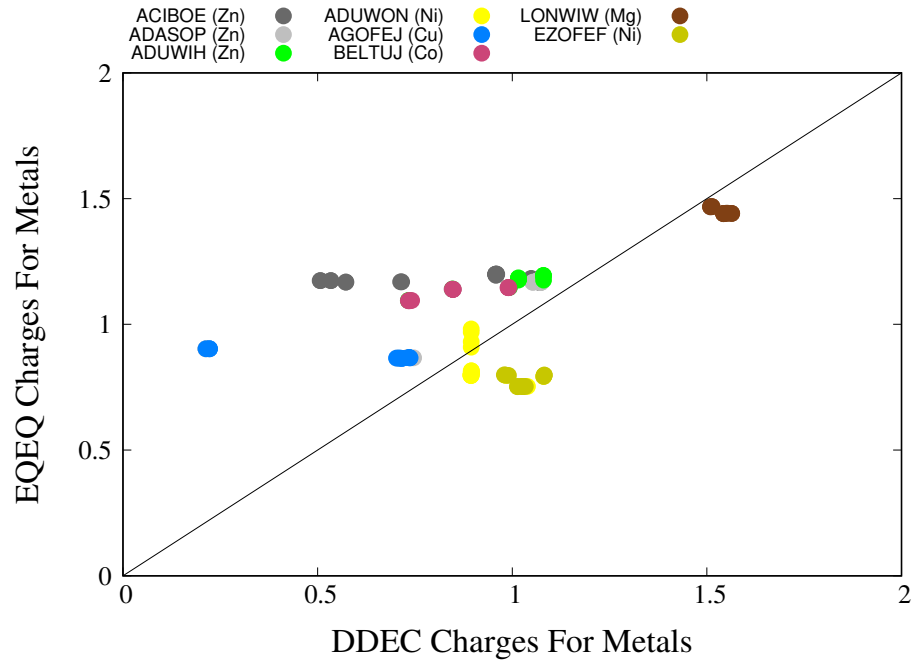

Figure 4.14. EQeq charges of metals in the studied Bio-MOFs compared with DDEC charges of metals.

Figure 4.15 shows the comparison of the EQeq and DDEC based charges of metal atoms in the Bio-MOFs. It can be seen that the charges of the metal atoms calculated by the EQeq method again fail to agree with the DDEC charges. The EQeq based charges of Co atoms of BELTUJ, Zn atoms of ACIBOE, ADASOP and ADUWIH and Cu atoms of AGOFEJ showed significant deviations from the charges calculated by the DDEC. However, point charges of the metal atoms of the remaining three Bio-MOFs (LONWIW, EZOFEF and ADUWON) give close results to the DDEC charges. It is important to note that those Bio-MOFs have the least amount of metal atoms in their unitcells, as reported in the Table 4.3.

5. CONCLUSIONS

5.1. Conclusion for the Accuracy of Permeability and Permeation Selectivity Calculation Methods

High throughput screening of MOFs for gas separation applications has been one of the recent research topics which has a potential to lead experimental studies. However, as we have showed in this paper, permeability formulations generally applied for determining membrane performances have raised accuracy and reliability concerns. We compare widely used permeability formulation, approximate method, and compare its results with the new method that is proposed previously by our group and detailed method which in principle gives correct results for gas permeabilities. H_2/CH_4 and CO_2/H_2 mixtures are selected as cases in order to examine the affects of purely LJ type (former) and electrostatic interactions (latter) on the predictions of the permeability formulations. Six ZIFs having different chemical and topological structures are selected as ZIF-6, ZIF-10, ZIF-60, ZIF-69, ZIF-79, and ZIF-81. Systematic comparison of three different methods give us the following results:

(1) For the H_2/CH_4 mixture, H_2 permeabilities using approximate and new methods accurately capture the results obtained using the detailed method. CH_4 permeabilities are predicted correctly by the approximate method only for the ZIFs having large pore sizes, e.g. ZIF-6, ZIF-10, and ZIF-60. For the ZIFs having relatively small pore sizes, ZIF-69, ZIF-79, and ZIF-81, approximate method results in moderate deviations from the correct results. The predictions of the new method, on the other hand, always improve the predictions of the approximate method for both component.

(2) For the CO_2/H_2 mixture, H_2 permeabilities using approximate and new methods significantly deviate from the detailed method only for ZIF-60 and ZIF-79. For the rest of the ZIFs, both methods capture the permeability trends of H_2. While ZIF-60 is considered as large pored ZIF, ZIF-79 has narrow pores as 4 Å. Thus, for the CO_2/H_2 mixture, type and strength of interactions between the gas molecules and ZIF pore surfaces affect the accuracy of permeability predictions, rather than only size of the pores. In the case of CO_2, however, both new and approximate methods fail to accurately reproduce the permeability values.

(3) For the gases having same kind of interactions with the materials, i.e. both H_2 and CH_4 interacting through dispersion interactions only, approximate and new methods both make good predictions for the fast diffusing component. For the heavier component, on the other hand, the new method significantly improves the predictions of the approximate method. The deviations obtained by the approximate method become even more significant for ZIFs having narrower pores.

(4) If the gas components interacting differently with the ZIFs, i.e. while H_2 is interacting only through LJ potential, CO_2 is interacting through both LJ and electrostatic interactions, new method makes better predictions than the approximate approach for the fast moving component. For the slowest component, on the other hand, both methods fail to capture the accurate results.

In conclusion, we question the accuracy of permeability formulations that are widely used in determining membrane performances especially for high throughput screening purposes. Our results raise the reliability concerns for the approximate method which can be significantly improved using the new method instead. For the components interacting through coulomb potential, on the other hand, the low accuracy results obtained by the new and approximate methods should be under consideration.

5.2. Conclusion of the Comparison of Charge Assignment Methods

The EQeq method shows notable deviations from the DDEC charges that assumed to be accurate. These deviations are observed clearly in the figures representing O, H, C and metal atomic point charges calculated using the DDEC and the EQeq.

Calculated H charges are mostly clustered in the graph but some indifferences can be also observed for some of the H atoms calculated by the EQeq with respect to the H charges calculated using the DDEC method. EQeq introduces special dielectric strength and a modified parameter to accurately calculate the atomic charges of the H atoms. This addition of parameters may improve the charge predictions of the method but the assumption does not

hold for all of the considered Bio-MOFs. From the literature review, it is known that the amount of H atoms in the internal areas of the structures affect the quality of the EQeq predictions due to usage of excessive amount of fitting parameters affecting the error rate negatively. Considering the results, it can be concluded that the EQeq method may not be trusted for the Bio-MOFs having large amount of H atoms.

The most significant dissimilarities observed between the DDEC and EQeq charges are the ones calculated for the O atoms. The reason can be attributed to the atomic environment that is neglected by the EQeq method. EQeq assigns the same electronegativity for all the O atoms in the framework, however electronegativity of an atom is not independent from it's nearby atomic environment, thus the O atoms in different locations of the structure might have distinct electronegativities and atomic charges. In addition, the number of metal atoms in the structure also affects the electronegativity. The Bio-MOFs having high metallic ratio shows larger deviations from the DDEC method. For most of the Bio-MOFs metallic atom charge calculations of the EQeq are not reliable compared to the DDEC charges.

As a conclusion, our results showed that the EQeq method fails to accurately calculate atomic charges compared to the DDEC method. EQeq-based charges give significant deviations from the DDEC charges for multiple common non-metal atoms (O, H and C) as well as several metal atoms. This deviations could lead to serious differences on partial charges and consequently influence the molecular simulations especially for the processes that are based on the degree of electrostatic interactions. We recommend that, although the EQeq method is fast and easy way to apply, the DDEC method should be used for properly characterizing adsorption and membrane based separation performances of the MOFs. Especially, for calculating the atomic charges of the Bio-MOFs having large number of metal atoms (metal ratio), the EQeq method should not be the first choice.

6. REFERENCES

1. Abdul Hamid, M. R., Shean Yaw, T. C., Mohd Tohir, M. Z., Wan Abdul Karim Ghani, W. A., Sutrisna, P. D., & Jeong, H.-K. (2021). Zeolitic imidazolate framework membranes for gas separations: Current state-of-the-art, challenges, and opportunities. *Journal of Industrial and Engineering Chemistry*, *98*, 17–41. https://doi.org/10.1016/j.jiec.2021.03.047

2. Altintas, C., Avci, G., Daglar, H., Gulcay, E., Erucar, I., & Keskin, S. (2018). Computer simulations of 4240 MOF membranes for H_2/CH_4 separations: Insights into structure–performance relations. *Journal of Materials Chemistry A*, *6*(14), 5836–5847. https://doi.org/10.1039/C8TA01547C

3. Altintas, C., & Keskin, S. (2019). Molecular Simulations of MOF Membranes and Performance Predictions of MOF/Polymer Mixed Matrix Membranes for CO2/CH4 Separations. *ACS Sustainable Chemistry & Engineering*, *7*(2), 2739–2750. https://doi.org/10.1021/acssuschemeng.8b05832

4. Altintas, C., & Keskin, S. (2020). Role of partial charge assignment methods in high-throughput screening of MOF adsorbents and membranes for CO_2/CH_4 separation. *Molecular Systems Design & Engineering*, *5*(2), 532–543. https://doi.org/10.1039/C9ME00163H

5. Andreoni, W. (2002). Density-Functional Theory and Molecular Dynamics: A New Perspective for Simulations of Biological Systems. In H. Kubinyi, G. Folkers, & Y. C. Martin (Eds.), *3D QSAR in Drug Design* (pp. 161–167). Dordrecht: Kluwer Academic Publishers. https://doi.org/10.1007/0-306-46857-3_9

6. Atci, E., Erucar, I., & Keskin, S. (2011). Adsorption and Transport of CH_4, CO_2, H_2 Mixtures in a Bio-MOF Material from Molecular Simulations. *The Journal of Physical Chemistry C*, *115*(14), 6833–6840. https://doi.org/10.1021/jp200429x

7. Atci, E., & Keskin, S. (2012a). Atomically Detailed Models for Transport of Gas Mixtures in ZIF Membranes and ZIF/Polymer Composite Membranes. *Industrial & Engineering Chemistry Research*, *51*(7), 3091–3100. https://doi.org/10.1021/ie202530f

8. Atci, E., & Keskin, S. (2012b). Understanding the Potential of Zeolite Imidazolate Framework Membranes in Gas Separations Using Atomically Detailed Calculations. *The Journal of Physical Chemistry C*, *116*(29), 15525–15537. https://doi.org/10.1021/jp305684d

9. *Atoms in Molecules: A Quantum Theory*. (1994). Oxford, New York: Oxford University Press.

10. Avci, G., Velioglu, S., & Keskin, S. (2018). High-Throughput Screening of MOF Adsorbents and Membranes for H_2 Purification and CO_2 Capture. *ACS Applied Materials & Interfaces*, *10*(39), 33693–33706. https://doi.org/10.1021/acsami.8b12746

11. Avci, G., Velioglu, S., & Keskin, S. (2019). In Silico Design of Metal Organic Frameworks with Enhanced CO_2 Separation Performances: Role of Metal Sites. *The Journal of Physical Chemistry C*, *123*(46), 28255–28265. https://doi.org/10.1021/acs.jpcc.9b08581

12. Babarao, R., Jiang, J., & Sandler, S. I. (2009). Molecular Simulations for Adsorptive Separation of CO_2 /CH_4 Mixture in Metal-Exposed, Catenated, and Charged Metal−Organic Frameworks. *Langmuir*, *25*(9), 5239–5247. https://doi.org/10.1021/la803074g

13. Banerjee, R., Furukawa, H., Britt, D., Knobler, C., O'Keeffe, M., & Yaghi, O. M. (2009). Control of Pore Size and Functionality in Isoreticular Zeolitic Imidazolate

Frameworks and their Carbon Dioxide Selective Capture Properties. *Journal of the American Chemical Society*, *131*(11), 3875–3877. https://doi.org/10.1021/ja809459e

14. Banerjee, R., Phan, A., Wang, B., Knobler, C., Furukawa, H., O'Keeffe, M., & Yaghi, O. M. (2008). High-throughput synthesis of zeolitic imidazolate frameworks and application to CO2 capture. *Science (New York, N.Y.)*, *319*(5865), 939–943. https://doi.org/10.1126/science.1152516

15. Baseden, K. A., & Tye, J. W. (2014). Introduction to Density Functional Theory: Calculations by Hand on the Helium Atom. *Journal of Chemical Education*, *91*(12), 2116–2123. https://doi.org/10.1021/ed5004788

16. Battisti, A., Taioli, S., & Garberoglio, G. (2011). Zeolitic imidazolate frameworks for separation of binary mixtures of CO2, CH4, N2 and H2: A computer simulation investigation. *Microporous and Mesoporous Materials*, *143*(1), 46–53. https://doi.org/10.1016/j.micromeso.2011.01.029

17. Breneman, C. M., & Wiberg, K. B. (1990). Determining atom-centered monopoles from molecular electrostatic potentials. The need for high sampling density in formamide conformational analysis. *Journal of Computational Chemistry*, *11*(3), 361–373. https://doi.org/10.1002/jcc.540110311

18. Buch, V. (1994). Path integral simulations of mixed para-D2 and ortho-D2 clusters: The orientational effects. *The Journal of Chemical Physics*, *100*(10), 7610–7629. https://doi.org/10.1063/1.466854

19. Bultinck, P., Van Alsenoy, C., Ayers, P. W., & Carbó-Dorca, R. (2007). Critical analysis and extension of the Hirshfeld atoms in molecules. *The Journal of Chemical Physics*, *126*(14), 144111. https://doi.org/10.1063/1.2715563

20. Cai, H., Huang, Y.-L., & Li, D. (2019). Biological metal–organic frameworks: Structures, host–guest chemistry and bio-applications. *Coordination Chemistry Reviews*, *378*, 207–221. https://doi.org/10.1016/j.ccr.2017.12.003

21. Campañá, C., Mussard, B., & Woo, T. K. (2009). Electrostatic Potential Derived Atomic Charges for Periodic Systems Using a Modified Error Functional. *Journal of Chemical Theory and Computation*, *5*(10), 2866–2878. https://doi.org/10.1021/ct9003405

22. Changlong Lin, Penley, D. R., Cho, E. H., & Lin, L.-C. (2020). Efficient and Accurate Charge Assignments via a Multilayer Connectivity-Based Atom Contribution (m-CBAC) Approach. *The Journal of Physical Chemistry C*, *124*(21), 11428–11437. https://doi.org/10.1021/acs.jpcc.0c01524

23. Chen, D.-L., Stern, A. C., Space, B., & Johnson, J. K. (2010). Atomic charges derived from electrostatic potentials for molecular and periodic systems. *The Journal of Physical Chemistry. A*, *114*(37), 10225–10233. https://doi.org/10.1021/jp103944q

24. Chokbunpiam, T., Fritzsche, S., Chmelik, C., Caro, J., Janke, W., & Hannongbua, S. (2016). Gate Opening, Diffusion, and Adsorption of CO2 and N2 Mixtures in ZIF-8. *The Journal of Physical Chemistry C*, *120*(41), 23458–23468. https://doi.org/10.1021/acs.jpcc.6b05506

25. Chung, Y. G., Haldoupis, E., Bucior, B. J., Haranczyk, M., Lee, S., Zhang, H., … Snurr, R. Q. (2019). Advances, Updates, and Analytics for the Computation-Ready, Experimental Metal–Organic Framework Database: CoRE MOF 2019. *Journal of Chemical & Engineering Data*, *64*(12), 5985–5998. https://doi.org/10.1021/acs.jced.9b00835

26. Colón, Y. J., Gómez-Gualdrón, D. A., & Snurr, R. Q. (2017). Topologically Guided, Automated Construction of Metal–Organic Frameworks and Their Evaluation for

Energy-Related Applications. *Crystal Growth & Design*, *17*(11), 5801–5810. https://doi.org/10.1021/acs.cgd.7b00848

27. D. C. Rapaport. (2004). *The Art of Molecular Dynamics Simulation*. Cambridge University Press. Retrieved from https://www.cambridge.org/core/books/art-of-molecular-dynamics-simulation/57D40C5ECE9B7EA17C0E77E7754F5874

28. Daglar, H., Erucar, I., & Keskin, S. (2021). Exploring the performance limits of MOF/polymer MMMs for O2/N2 separation using computational screening. *Journal of Membrane Science*, *618*, 118555. https://doi.org/10.1016/j.memsci.2020.118555

29. Dantu, S. (2012). *Conformational sampling of enzyme dynamics: Triosephosphate isomerase*.

30. Deeg, K. S., Gutiérrez-Sevillano, J. J., Bueno-Pérez, R., Parra, J. B., Ania, C. O., Doblaré, M., & Calero, S. (2013). Insights on the Molecular Mechanisms of Hydrogen Adsorption in Zeolites. *The Journal of Physical Chemistry C*, *117*(27), 14374–14380. https://doi.org/10.1021/jp4037233

31. Düren, T., Sarkisov, L., Yaghi, O. M., & Snurr, R. Q. (2004). Design of New Materials for Methane Storage. *Langmuir*, *20*(7), 2683–2689. https://doi.org/10.1021/la0355500

32. Düren, T., & Snurr, R. Q. (2004). Assessment of Isoreticular Metal−Organic Frameworks for Adsorption Separations: A Molecular Simulation Study of Methane/n-Butane Mixtures. *The Journal of Physical Chemistry B*, *108*(40), 15703–15708. https://doi.org/10.1021/jp0477856

33. Durğun, Y. G. (2019). *Computational Assessment of Zeolitic-Imidazolate Frameworks (ZIFs) for Adsorption and Diffusion Based Separation of Noble Gas Mixtures*. 10.

34. Erucar, I., & Keskin, S. (2015). Computational Modeling of bio-MOFs for CO2/CH4 separations. *Chemical Engineering Science*, *130*, 120–128. https://doi.org/10.1016/j.ces.2015.03.016

35. Erucar, I., Manz, T. A., & Keskin, S. (2014). Effects of electrostatic interactions on gas adsorption and permeability of MOF membranes. *Molecular Simulation*, *40*(7–9), 557–570. https://doi.org/10.1080/08927022.2013.829219

36. Evans, D. J., & Holian, B. L. (1985). The Nose–Hoover thermostat. *The Journal of Chemical Physics*, *83*(8), 4069–4074. https://doi.org/10.1063/1.449071

37. First, E., & Floudas, C. (2013). MOFomics: Computational pore characterization of metal–organic frameworks. *Microporous and Mesoporous Materials*, *165*, 32–39. https://doi.org/10.1016/j.micromeso.2012.07.049

38. Fischer, M., Hoffmann, F., & Fröba, M. (2012). Metal–organic frameworks and related materials for hydrogen purification: Interplay of pore size and pore wall polarity. *RSC Advances*, *2*(10), 4382. https://doi.org/10.1039/c2ra01239a

39. Frenkel, D., & Smit, B. (1996). Understanding molecular simulation: From algorithms to applications. 2nd ed. In *Physics Today* (Vol. 50). https://doi.org/10.1063/1.881812

40. Gagliardi, L., Lindh, R., & Karlström, G. (2004). Local properties of quantum chemical systems: The LoProp approach. *The Journal of Chemical Physics*, *121*(10), 4494. (world). https://doi.org/10.1063/1.1778131

41. Glover, J., & Besley, E. (2021). A high-throughput screening of metal–organic framework based membranes for biogas upgrading. *Faraday Discussions*, *231*, 235–257. https://doi.org/10.1039/D1FD00005E

42. Guo, H., Shi, F., Ma, Z., & Liu, X. (2010). Molecular Simulation for Adsorption and Separation of CH4/H2 in Zeolitic Imidazolate Frameworks. *The Journal of Physical Chemistry C*, *114*(28), 12158–12165. https://doi.org/10.1021/jp908978q

43. Gurdal, Y. (2019). *Computational Assessment of Zeolitic-Imidazolate Frameworks (ZIFs) forAdsorption and Diffusion Based Separation of Noble Gas Mixtures*. *8*, 1009–1018.

44. Gurdal, Y. (2021). Theoretical investigation of ZIFs as adsorbents or membranes for separating noble gas mixtures: Applying a newer method for predicting performances. *Journal of Porous Materials*, *28*(3), 905–917. https://doi.org/10.1007/s10934-021-01045-9

45. Gurdal, Y., & Keskin, S. (2016). A new approach for predicting gas separation performances of MOF membranes. *Journal of Membrane Science*, *519*, 45–54. https://doi.org/10.1016/j.memsci.2016.07.039

46. Haldoupis, E., Nair, S., & Sholl, D. S. (2012). Finding MOFs for Highly Selective CO2/N2 Adsorption Using Materials Screening Based on Efficient Assignment of Atomic Point Charges. *Journal of the American Chemical Society*, *134*(9), 4313–4323. https://doi.org/10.1021/ja2108239

47. Han, S. S., Choi, S.-H., & Goddard, W. A. (2010). Zeolitic Imidazolate Frameworks as H_2 Adsorbents: Ab Initio Based Grand Canonical Monte Carlo Simulation. *Journal of Physical Chemistry C*, *114*(27), 12039–12047.

48. Henkelman, G., Arnaldsson, A., & Jónsson, H. (2006). A fast and robust algorithm for Bader decomposition of charge density. *Computational Materials Science*, *36*(3), 354–360. https://doi.org/10.1016/j.commatsci.2005.04.010

49. Hirshfeld, F. L. (1977). Bonded-atom fragments for describing molecular charge densities. *Theoretica Chimica Acta*. https://doi.org/10.1007/BF00549096

50. Home - The Cambridge Crystallographic Data Centre (CCDC). (n.d.). Retrieved 28 November 2021, from https://www.ccdc.cam.ac.uk/

51. Huang, C., Li, C., Choi, P. Y. K., Nandakumar, K., & Kostiuk, L. W. (2010). Effect of cut-off distance used in molecular dynamics simulations on fluid properties. *Molecular Simulation*, *36*(11), 856–864. https://doi.org/10.1080/08927022.2010.489556

52. Hwang, S.-T. (2004). Nonequilibrium thermodynamics of membrane transport. *AIChE Journal*, *50*(4), 862–870. https://doi.org/10.1002/aic.10082

53. Jung, D. H., Kim, D., Lee, T. B., Choi, S. B., Yoon, J. H., Kim, J., … Choi, S.-H. (2006). Grand Canonical Monte Carlo Simulation Study on the Catenation Effect on Hydrogen Adsorption onto the Interpenetrating Metal−Organic Frameworks. *The Journal of Physical Chemistry B*, *110*(46), 22987–22990. https://doi.org/10.1021/jp065819z

54. Keskin, S. (2010). Comparing Performance of CPO and IRMOF Membranes for Gas Separations Using Atomistic Models. *Industrial & Engineering Chemistry Research*, *49*(22), 11689–11696. https://doi.org/10.1021/ie1015443

55. Keskin, S. (2011). Atomistic Simulations for Adsorption, Diffusion, and Separation of Gas Mixtures in Zeolite Imidazolate Frameworks. *The Journal of Physical Chemistry C*, *115*(3), 800–807. https://doi.org/10.1021/jp109743e

56. Keskin, S. (2013). Gas adsorption and diffusion in a highly CO2 selective metal–organic framework: Molecular simulations. *Molecular Simulation*, *39*(1), 14–24. https://doi.org/10.1080/08927022.2012.700485

57. Keskin, S., & Sholl, D. S. (2009). Efficient Methods for Screening of Metal Organic Framework Membranes for Gas Separations Using Atomically Detailed Models. *Langmuir*, *25*(19), 11786–11795. https://doi.org/10.1021/la901438x

58. Krishna, R., & van Baten, J. M. (2007). Using molecular simulations for screening of zeolites for separation of CO2/CH4 mixtures. *Chemical Engineering Journal*, *133*(1–3), 121–131. https://doi.org/10.1016/j.cej.2007.02.011

59. Krishna, Rajamani, & Baten, J. (2011). Investigating the potential of MgMOF-74 membranes for CO2 capture. *Journal of Membrane Science*, *377*, 249–260. https://doi.org/10.1016/j.memsci.2011.05.001

60. Krishna, Rajamani, & van Baten, J. M. (2010). In silico screening of zeolite membranes for CO₂ capture. *Journal of Membrane Science*, *360*(1–2), 323–333.

61. Krykunov, M., Demone, C., Lo, J. W.-H., & Woo, T. K. (2017). A New Split Charge Equilibration Model and REPEAT Electrostatic Potential Fitted Charges for Periodic Frameworks with a Net Charge. *Journal of Chemical Theory and Computation*, *13*(6), 2858–2869. https://doi.org/10.1021/acs.jctc.6b00998

62. Kühne, T. D., Iannuzzi, M., Del Ben, M., Rybkin, V. V., Seewald, P., Stein, F., … Hutter, J. (2020). CP2K: An electronic structure and molecular dynamics software package - Quickstep: Efficient and accurate electronic structure calculations. *The Journal of Chemical Physics*, *152*(19), 194103. https://doi.org/10.1063/5.0007045

63. Li, D., Chen, L., Liu, G., Yuan, Z., Li, B., Zhang, X., & Wei, J. (2021). Porous metal–organic frameworks for methane storage and capture: Status and challenges. *New Carbon Materials*, *36*(3), 468–496. https://doi.org/10.1016/S1872-5805(21)60034-3

64. Li, L., Wang, Y., Yang, J., Wang, X., & Li, J. (2015). Targeted capture and pressure/temperature-responsive separation in flexible metal–organic frameworks. *Journal of Materials Chemistry A, 3*(45), 22574–22583. https://doi.org/10.1039/C5TA00679A

65. Li, S., Chung, Y. G., & Snurr, R. Q. (2016). High-Throughput Screening of Metal–Organic Frameworks for CO_2 Capture in the Presence of Water. *Langmuir*, *32*(40), 10368–10376. https://doi.org/10.1021/acs.langmuir.6b02803

66. Li, W., Xia, X., & Li, S. (2020). Screening of Covalent–Organic Frameworks for Adsorption Heat Pumps. *ACS Applied Materials & Interfaces*, *12*(2), 3265–3273. https://doi.org/10.1021/acsami.9b20837

67. Limas, N., & Manz, T. (2018). Introducing DDEC6 atomic population analysis: Part 4. Efficient parallel computation of net atomic charges, atomic spin moments, bond orders, and more. *RSC Advances, 8*, 2678–2707. https://doi.org/10.1039/C7RA11829E

68. Liu, D., & Zhong, C. (2010). Understanding gas separation in metal–organic frameworks using computer modeling. *Journal of Materials Chemistry, 20*(46), 10308–10318. https://doi.org/10.1039/C0JM01045F

69. Liu, Y., Hu, E., Khan, E. A., & Lai, Z. (2010). Synthesis and characterization of ZIF-69 membranes and separation for CO2/CO mixture. *Journal of Membrane Science*, *353*(1–2), 36–40. https://doi.org/10.1016/j.memsci.2010.02.023

70. Lj-cutoff-scheme.svg—Wikibooks, open books for an open world. (2019, May 22). Retrieved 5 December 2021, from Molecular Simulation/Treatment of Long Range Forces website: https://en.wikibooks.org/wiki/Molecular_Simulation/Treatment_of_Long_Range_Forces

71. Maginn, E. J., Bell, A. T., & Theodorou, D. N. (1993). Transport diffusivity of methane in silicalite from equilibrium and nonequilibrium simulations. *The Journal of Physical Chemistry*, *97*(16), 4173–4181. https://doi.org/10.1021/j100118a038

72. Manz, T. A., & Sholl, D. S. (2010). Chemically Meaningful Atomic Charges That Reproduce the Electrostatic Potential in Periodic and Nonperiodic Materials. *Journal of Chemical Theory and Computation*, *6*(8), 2455–2468. https://doi.org/10.1021/ct100125x

73. Martin, M. G., & Siepmann, J. I. (1998). Transferable Potentials for Phase Equilibria. 1. United-Atom Description of n-Alkanes. *The Journal of Physical Chemistry B*, *102*(14), 2569–2577. https://doi.org/10.1021/jp972543+

74. Mayo, S. L., Olafson, B. D., & Goddard, W. (1990). *DREIDING: A generic force field for molecular simulations*. https://doi.org/10.1021/J100389A010

75. Metropolis, N., Rosenbluth, A. W., Rosenbluth, M. N., Teller, A. H., & Teller, E. (1953). Equation of State Calculations by Fast Computing Machines. *The Journal of Chemical Physics*, *21*(6), 1087–1092. https://doi.org/10.1063/1.1699114

76. Nazarian, D., Camp, J. S., & Sholl, D. S. (2016). A Comprehensive Set of High-Quality Point Charges for Simulations of Metal–Organic Frameworks. *Chemistry of Materials*, *28*(3), 785–793. https://doi.org/10.1021/acs.chemmater.5b03836

77. Ongari, D., Boyd, P. G., Kadioglu, O., Mace, A. K., Keskin, S., & Smit, B. (2019). Evaluating Charge Equilibration Methods To Generate Electrostatic Fields in Nanoporous Materials. *Journal of Chemical Theory and Computation*, *15*(1), 382–401. https://doi.org/10.1021/acs.jctc.8b00669

78. Onsager, L. (1931). Reciprocal Relations in Irreversible Processes. I. *Physical Review*, *37*(4), 405–426. https://doi.org/10.1103/PhysRev.37.405

79. Panahi, Y., Mellatyar, H., Farshbaf, M., Sabet, Z., Fattahi, T., & Akbarzadehe, A. (2018). Biotechnological applications of nanomaterials for air pollution and water/wastewater treatment. *Materials Today: Proceedings*, *5*(7), 15550–15558. https://doi.org/10.1016/j.matpr.2018.04.162

80. Park, K. S., Ni, Z., Côté, A. P., Choi, J. Y., Huang, R., Uribe-Romo, F. J., … Yaghi, O. M. (2006). Exceptional chemical and thermal stability of zeolitic imidazolate frameworks. *Proceedings of the National Academy of Sciences of the United States of America*, *103*(27), 10186–10191. https://doi.org/10.1073/pnas.0602439103

81. Pérez-Pellitero, J., Amrouche, H., Siperstein, F. R., Pirngruber, G., Nieto-Draghi, C., Chaplais, G., … Bats, N. (2010). Adsorption of CO2, CH4, and N2 on Zeolitic Imidazolate Frameworks: Experiments and Simulations. *Chemistry – A European Journal*, *16*(5), 1560–1571. https://doi.org/10.1002/chem.200902144

82. Qiao, Z., Xu, Q., & Jiang, J. (2018). High-throughput computational screening of metal-organic framework membranes for upgrading of natural gas. *Journal of Membrane Science*, *551*, 47–54. https://doi.org/10.1016/j.memsci.2018.01.020

83. Rappe, A. K., Casewit, C. J., Colwell, K. S., Goddard, W. A., & Skiff, W. M. (1992). UFF, a full periodic table force field for molecular mechanics and molecular dynamics simulations. *Journal of the American Chemical Society*, *114*(25), 10024–10035. https://doi.org/10.1021/ja00051a040

84. Rappe, Anthony K., & Goddard, W. A. (1991). Charge equilibration for molecular dynamics simulations. *The Journal of Physical Chemistry*, *95*(8), 3358–3363. https://doi.org/10.1021/j100161a070

85. Sanborn, M. J., & Snurr, R. Q. (2001). Predicting membrane flux of CH4 and CF4 mixtures in Faujasite from molecular simulations. *AIChE Journal*, *47*(9), 2032–2041. https://doi.org/10.1002/aic.690470914

86. Skoulidas, A., Bowen, T., Doelling, C. M., Falconer, J., Noble, R., & Sholl, D. (2003). *Comparing atomistic simulations and experimental measurements for CH4/CF4 mixture permeation through silicalite membranes*. *227*, 123–136. https://doi.org/10.1016/J.MEMSCI.2003.08.021

87. Sladekova, K., Campbell, C., Grant, C., Fletcher, A. J., Gomes, J. R. B., & Jorge, M. (2021). Correction to: The effect of atomic point charges on adsorption isotherms of CO2 and water in metal organic frameworks. *Adsorption*, *27*(6), 995–1000. https://doi.org/10.1007/s10450-021-00301-3

88. Sumer, Z., & Keskin, S. (2017). Molecular Simulations of MOF Adsorbents and Membranes for Noble Gas Separations. *Chemical Engineering Science*, *164*. https://doi.org/10.1016/j.ces.2017.02.010

89. Sun, H., Jiang, H., Kong, R., Ren, D., Wang, D., Tan, J., … Shen, B. (2019). Tuning *n* -Alkane Adsorption on Mixed-Linker Zeolitic Imidazolate Framework-8-90 via Controllable Ligand Hybridization: Insight into the Confinement from an Energetics Perspective. *Industrial & Engineering Chemistry Research*, *58*(29), 13274–13283. https://doi.org/10.1021/acs.iecr.9b00941

90. Tan, J. C., & Cheetham, A. K. (2011). Mechanical properties of hybrid inorganic–organic framework materials: Establishing fundamental structure–property relationships. *Chemical Society Reviews*, *40*(2), 1059. https://doi.org/10.1039/c0cs00163e

91. Verlet, L. (1967). Computer ‘Experiments’ on Classical Fluids. I. Thermodynamical Properties of Lennard-Jones Molecules. *Physical Review*, *159*(1), 98–103. https://doi.org/10.1103/PhysRev.159.98

92. Verma, S., Mishra, A. K., & Kumar, J. (2010). The Many Facets of Adenine: Coordination, Crystal Patterns, and Catalysis. *Accounts of Chemical Research*, *43*(1), 79–91. https://doi.org/10.1021/ar9001334

93. Walton, K. S., Millward, A. R., Dubbeldam, D., Frost, H., Low, J. J., Yaghi, O. M., & Snurr, R. Q. (2008). Understanding Inflections and Steps in Carbon Dioxide Adsorption Isotherms in Metal-Organic Frameworks. *Journal of the American Chemical Society*, *130*(2), 406–407. https://doi.org/10.1021/ja076595g

94. Wang, B., Côté, A. P., Furukawa, H., O’Keeffe, M., & Yaghi, O. M. (2008). Colossal cages in zeolitic imidazolate frameworks as selective carbon dioxide reservoirs. *Nature*, *453*(7192), 207–211. https://doi.org/10.1038/nature06900

95. Watanabe, T., Manz, T. A., & Sholl, D. S. (2011). Accurate Treatment of Electrostatics during Molecular Adsorption in Nanoporous Crystals without Assigning Point Charges to Framework Atoms. *The Journal of Physical Chemistry C*, *115*(11), 4824–4836. https://doi.org/10.1021/jp201075u

96. Watanabe, T., & Sholl, D. S. (2012). Accelerating Applications of Metal–Organic Frameworks for Gas Adsorption and Separation by Computational Screening of Materials. *Langmuir*, *28*(40), 14114–14128. https://doi.org/10.1021/la301915s

97. Wilmer, C. E., Farha, O. K., Bae, Y.-S., Hupp, J. T., & Snurr, R. Q. (2012). Structure–property relationships of porous materials for carbon dioxide separation and capture. *Energy & Environmental Science*, *5*(12), 9849. https://doi.org/10.1039/c2ee23201d

98. Wilmer, C. E., Kim, K. C., & Snurr, R. Q. (2012). An Extended Charge Equilibration Method. *The Journal of Physical Chemistry Letters*, *3*(17), 2506–2511. https://doi.org/10.1021/jz3008485

99. WwPDB: Worldwide Protein Data Bank. (n.d.). Retrieved 28 November 2021, from https://www.wwpdb.org/

100. Xu, Q., & Zhong, C. (2010). A General Approach for Estimating Framework Charges in Metal−Organic Frameworks. *The Journal of Physical Chemistry C*, *114*(11), 5035–5042. https://doi.org/10.1021/jp910522h

101. Yaghi, O. M., Li, G., & Li, H. (1995). Selective binding and removal of guests in a microporous metal–organic framework. *Nature*, *378*(6558), 703–706. https://doi.org/10.1038/378703a0

102. Yang, Q., Xue, C., Zhong, C., & Chen, J.-F. (2007). Molecular simulation of separation of CO2 from flue gases in CU-BTC metal-organic framework. *AIChE Journal*, *53*(11), 2832–2840. https://doi.org/10.1002/aic.11298

103. Yang, Q., & Zhong, C. (2006). Electrostatic-Field-Induced Enhancement of Gas Mixture Separation in Metal-Organic Frameworks: A Computational Study. *ChemPhysChem*, *7*(7), 1417–1421. https://doi.org/10.1002/cphc.200600191

104. Yilmaz, G., Ozcan, A., & Keskin, S. (2015). Computational screening of ZIFs for CO2 separations. *Molecular Simulation*, *41*(9), 713–726. https://doi.org/10.1080/08927022.2014.923568

105. Zang, J., Nair, S., & Sholl, D. S. (2013). Prediction of Water Adsorption in Copper-Based Metal–Organic Frameworks Using Force Fields Derived from Dispersion-Corrected DFT Calculations. *The Journal of Physical Chemistry C*, *117*(15), 7519–7525. https://doi.org/10.1021/jp310497u

106. Zeeshan, M., Nozari, V., Yagci, M. B., Isık, T., Unal, U., Ortalan, V., … Uzun, A. (2018). Core–Shell Type Ionic Liquid/Metal Organic Framework Composite: An Exceptionally High CO2/CH4 Selectivity. *Journal of the American Chemical Society*, *140*(32), 10113–10116. https://doi.org/10.1021/jacs.8b05802

107.Zeng, H., Liu, Y., & Liu, H. (2018). Adsorption and diffusion of CO2 and CH4 in covalent organic frameworks: An MC/MD simulation study. *Molecular Simulation*, *44*(15), 1244–1251. https://doi.org/10.1080/08927022.2018.1481959

108. Zhang, K., Zhang, L., & Jiang, J. (2013). Adsorption of C1–C4 Alcohols in Zeolitic Imidazolate Framework-8: Effects of Force Fields, Atomic Charges, and Framework Flexibility. *The Journal of Physical Chemistry C*, *117*(48), 25628–25635. https://doi.org/10.1021/jp409869c

109.Zheng, B., Sant, M., Demontis, P., & Suffritti, G. B. (2012). Force Field for Molecular Dynamics Computations in Flexible ZIF-8 Framework. *The Journal of Physical Chemistry C*, *116*(1), 933–938. https://doi.org/10.1021/jp209463a

110.Zheng, C., Liu, D., Yang, Q., Zhong, C., & Mi, J. (2009). Computational Study on the Influences of Framework Charges on CO2 Uptake in Metal−Organic Frameworks. *Industrial & Engineering Chemistry Research*, *48*(23), 10479–10484. https://doi.org/10.1021/ie901000x

111.Zielinski, J. M., & Alsoy, S. (2001). Onsager consistency checks for multicomponent diffusion models. *Journal of Polymer Science Part B: Polymer Physics*, *39*(13), 1496–1504. https://doi.org/10.1002/polb.1121